Supplementary Information for:

On the appearance of nitrite anion in [PdX(OAc)L_2] and [Pd(X)(C^N)L] syntheses (X = OAc or NO_2): photocrystallographic identification of metastable Pd(η^1-ONO)(C^N)PPh_3

Somia E. Bajwa,[a] Thomas E. Storr,[a,b] Lauren E. Hatcher,[c] Thomas J. Williams,[a] Christoph G. Baumann,[b] Adrian C. Whitwood,[a] David R. Allan,[d] Simon J. Teat,[e] Paul R. Raithby[c] and Ian J. S. Fairlamb[a]**

[a] *Department of Chemistry, University of York, York, YO10 5DD, UK. Fax: 0044 (0)1904 322516; Tel: 0044 324091; E-mail: ian.fairlamb@york.ac.uk*

[b] *Department of Biology, University of York, York, YO10 5DD, UK. Tel: 0044 (0)1904 328828.*

[c] *Department of Chemistry, University of Bath, Bath, BA2 7AY, UK.*

Fax: 0044 (0)1225 383 183; E-mail: p.r.raithby@bath.ac.uk

[d] *Diamond Light Source Ltd, Diamond House, Harwell Science and Innovation Campus, Didcot, Oxfordshire OX11 0DE.*

[e] *Advanced Light Source, Lawrence Berkeley National Laboratory, Berkeley, Berkeley, CA 94720-8229, USA.*

Contents:

Continued:

1. General information

1.1. Preparative and laboratory analysis

Dry and degassed acetonitrile and dichloromethane were obtained from a Pure Solv MD-7 solvent purification system. 'Dry' dimethyl sulfoxide was obtained from Acros (99.7+% extra dry over molecular sieves). Acetonitrile used some reactions (indicated below in individual reactions) was dried and purified by triply distilling over anhydrous $AlCl_3$, then Li_2CO_3 and finally CaH_2, according to a procedure reported by Walter and Ramaley (*method A*).[1] Nitrogen gas was oxygen-free and dried immediately prior to use by passage through a column containing sodium hydroxide pellets and silica. Commercial chemicals were purchased from Sigma-Aldrich or Alfa Aesar.

All air sensitive procedures were carried out using Schlenk techniques (high vacuum, liquid nitrogen trap on a standard in-house built dual line). Where necessary a glove (dry) box was used (<0.5 ppm O_2). Room temperature upper and lower limits are stated as 13-25 °C, but typically 21 °C was recorded. Commercial chemicals were purchased from Sigma-Aldrich and Alfa Aesar and used directly unless otherwise stated in the text. Brine refers to a saturated aqueous solution of NaCl.

TLC analysis was carried out on Merck TLC aluminium sheets (silica gel 60 F254) and visualised with UV light (at 254 nm), iodine vapour or an aqueous solution of potassium permanganate. Flash chromatography was run on silica gel 60 according to the method reported by W. C. Still *et al.*[2]
Melting points were recorded using a Stuart digital SMP3 machine and are uncorrected values.

1.2. Instrument details for compound characterisation purposes:

NMR spectra were obtained in the solvent indicated, using a JEOL ECX400 or JEOL ECS400 spectrometer (400MHz, 101 MHz and 162 MHz for ^{1}H, ^{13}C and ^{31}P, respectively), or a Bruker 500 (500 MHz, 126 MHz and 202 MHz for ^{1}H, ^{13}C and ^{31}P, respectively). Chemical shifts are reported in parts per million and were referenced to the residual undeuterated solvent of the deuterated solvent used ($CHCl_3$ δ_H = 7.26 and δ_C = 77.16 ($CDCl_3$), $CDHCl_2$ δ_H = 5.31 and δ_C = 54.0 (CD_2Cl_2), $(CHD_2)SO(CD_3)$ δ_H = 2.50 and δ_C = 39.52 {$SO(CD_3)_2$}, ^{1}H and ^{13}C, respectively). Spectra were typically run at a temperature of 300 K. All ^{13}C NMR spectra were obtained with ^{1}H decoupling. ^{31}P NMR were externally referenced to H_3PO_4, and recorded with ^{1}H decoupling. NMR spectra were processed using MestrNova software (versions 5.3 and 7.03). The spectra given below were saved as either .BMP or .PNG files in MestrNova and inserted directly into a Microsoft Word Document. For the ^{1}H NMR spectra the resolution varies from 0.15 to 0.5 Hz; the coupling constants have been quoted to ±0.5 Hz in all cases for consistency. ^{1}H NMR chemical shifts are quoted to 2 decimal places; ^{13}C and ^{31}P NMR chemical shifts are quoted to 1

decimal place (note: for some ^{13}C signals it was necessary to quote 2 decimal places). Numbers were rounded to the nearest value, *e.g.* 1.237 ≈ 1.24, 1.232 ≈ 1.23.

IR spectroscopy was undertaken using a Jasco/MIRacle FT/IR-4100typeA spectrometer using an ATR attachment on solid and liquid compounds; solution and KBr (disc) IR spectra were obtained on a Nicolet Avatar 370 FT-IR spectrometer, according to standard procedures.

MS spectra were measured using a Bruker Daltronics micrOTOF MS, Agilent series 1200LC with electrospray ionisation (ESI and APCI) or on a Thermo LCQ using electrospray ionisation, with <5 ppm error recorded for all HRMS samples. LIFDI mass spectrometry was carried out using a Waters GCT Premier MS Agilent 7890A GC (usually for analysis of organometallic compounds when ESI or APCI are not satisfactory ionisation methods). Mass spectral data is quoted as the *m/z* ratio along with the relative peak height in brackets (base peak = 100).

UV-visible spectra were recorded using a JASCO V-560 instrument with quartz cells (1 cm path length). Spectra were processed in SigmaPlot version 10.0 (2006 Systat Software, Inc.).

2. Characterisation of "$Pd(OAc)_2$" samples

2.1. Commercial sources of $Pd_3(OAc)_6$: Analysis

^1H NMR spectrum for some commercially available '$Pd(OAc)_2$' sources (found in Chemistry laboratories at the University of York) obtained using reagent grade $CDCl_3$ (*e.g.* wet). For reference purposes 75% and 95% $Pd_3(OAc)_5NO_2$ spectra are also included.

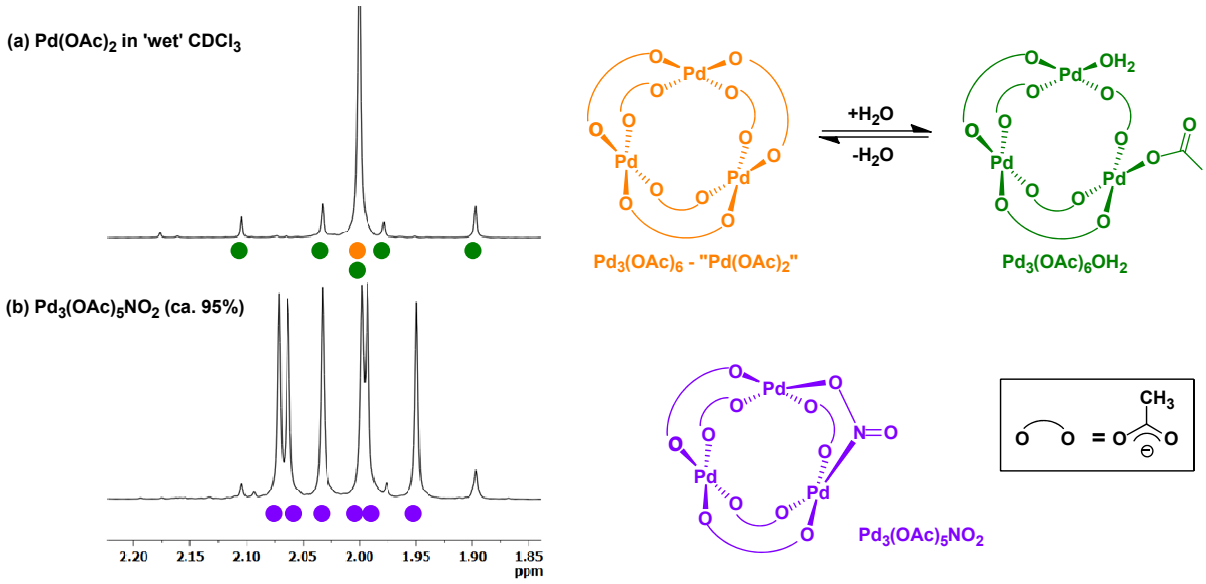

Figure 1: ^1H NMR spectra of pure "$Pd(OAc)_2$" and $Pd_3(OAc)_5NO_2$ (*ca.* 95%) (400 MHz).

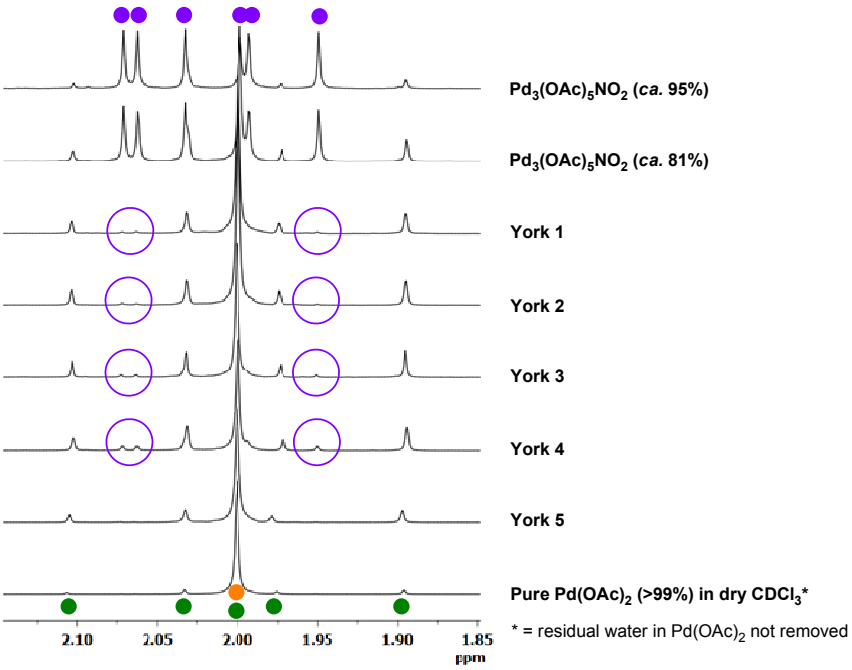

Figure 2: ^{1}H NMR spectra of various commercial batches of "$Pd(OAc)_2$" found in the Chemistry Laboratories at the University of York (*using reagent grade 'wet' $CDCl_3$ unless otherwise specified*) (400 MHz). The purple circles highlight trace $Pd_3(OAc)_5NO_2$. For reference purposes, ^{1}H NMR spectra of $Pd_3(OAc)_5NO_2$ (*ca.* 95% and 81% purity materials) and pure $Pd(OAc)_2$ in dry $CDCl_3$ are included.

2.1.1. Elemental Analysis of Impure palladium(II) acetate, $Pd_3(OAc)_5NO_2$

		% C	% H	% N
Observed	Impure material Pd material	18.47	2.24	1.72
Calculated	$Pd_3(OAc)_5NO_2$	18.18	2.29	2.12
Calculated	$Pd_3(OAc)_6$	21.40	2.69	-

- % $Pd_3(OAc)_5NO_2$ (based on nitrogen content) = (1.72/2.12)x100 = <u>81.13%</u>

2.1.1.1. Ratio of NO_2:OAc in 81% $Pd_3(OAc)_5NO_2$

- Ratio of $Pd_3(OAc)_5NO_2$:$Pd_3(OAc)_6$ = 81.13:18.87 = <u>4.3:1</u>
- Total (relative) OAc content =

  4.3x5 OAc {from ($Pd_3(OAc)_5NO_2$}
  6 OAc {from $Pd_3(OAc)_6$}
  Total = <u>27.5 OAc</u>

- Total (relative) NO_2 content =

  <u>4.3 NO_2</u> {from ($Pd_3(OAc)_5NO_2$}

- Ratio of OAc:NO_2 = 27.5:4.3 = <u>6.4:1</u>

3. Synthesis and Characterisation of $Pd(OAc)(NO_2)(pip)_2$ and $Pd(OAc)_2(pip)_2$ complexes

3.1. *bis-trans*-{*N*(H)-piperidinyl}palladium(II) acetate [$Pd(OAc)_2(pip)_2$]

To a N_2-flushed vacuum dried Schlenk tube was added $Pd(OAc)_2$ (112 mg, 0.5 mmol, 1.0 eq.) and THF (5 ml) which was then stirred under N_2 atmosphere until fully dissolved. To this solution, piperidine (99 µl, 1.0 mmol, 2.0 eq.) was added dropwise by syringe (*via* a SubaSeal®), and the reaction was stirred at room temperature for 5 minutes. The solvent was then removed *in vacuo* to yield a light yellow solid (163 mg, 83%). The complex can be recrystallised from CH_2Cl_2:hexane (2:1, *v/v*) at *ca.* -18 °C to prevent precipitation of palladium black. ^{1}H NMR (400 MHz, $CDCl_3$) δ 5.50 (t, *J* = 11.9 Hz, 2H), 3.14 (d, *J* = 12.2 Hz, 4H), 2.56 (qd, *J* = 2.8, 12.2 Hz, 4H), 1.95 (s, 6H), 1.75-1.56 (m, 6H), 1.51-1.30 (m, 6H); ^{13}C NMR (101.6 MHz, $CDCl_3$) δ 180.4, 49.2, 26.5, 24.0, 23.8; LIFDI MS, *m/z* 394 [100 % $(M)^+$] and correct isotopic distribution; Elemental Analysis, Calcd. for $C_{14}H_{28}O_4N_2.(H_2O)_{0.5}$ (found) %: C 41.74 (41.43), H 7.01 (6.90), N 6.95 (7.25).

3.2. *bis-trans*-{*N*(H)-piperidinyl}palladium(II) nitroacetate [$Pd(OAc)(NO_2)(pip)_2$]

Using an impure batch of $Pd(OAc)_2$ (*ca.* 81% $Pd_3(OAc)_5NO_2$) the above procedure (Section 3.1) was used. Crystallisation of the mixture of the two complexes formed (see NMR spectra below) from CH_2Cl_2:hexane (1:1, *v/v*) at -18 °C yielded [$Pd(OAc)_2(pip)_2$] as a yellow powder, and [$Pd(OAc)(NO_2)(pip)_2$] as large yellow crystals which were seperated manually by using hand tweezers. ^{1}H NMR (400 MHz, $CDCl_3$) δ 4.22 (t, *J* = 12.3 Hz, 2H), 3.28 (dt, *J* = 14.8, 1.7 Hz, 4H), 2.75 (qd, *J* = 12.5, 2.9 Hz, 4H), 1.99 (s, 3H), 1.74–1.63 (m, 6H), 1.58–1.38 (m, 6H); ^{13}C NMR (101 MHz, $CDCl_3$) δ 179.1, 50.6, 27.1, 24.2, 23.6; LIFDI MS, *m/z* 381 [100 % $(M)^+$] and correct isotopic distribution; Elemental Analysis, Calcd. for $C_{12}H_{25}O_4N_3$ (found) %: C 37.76 (37.66), H 6.60 (6.44), N 11.01 (10.64).

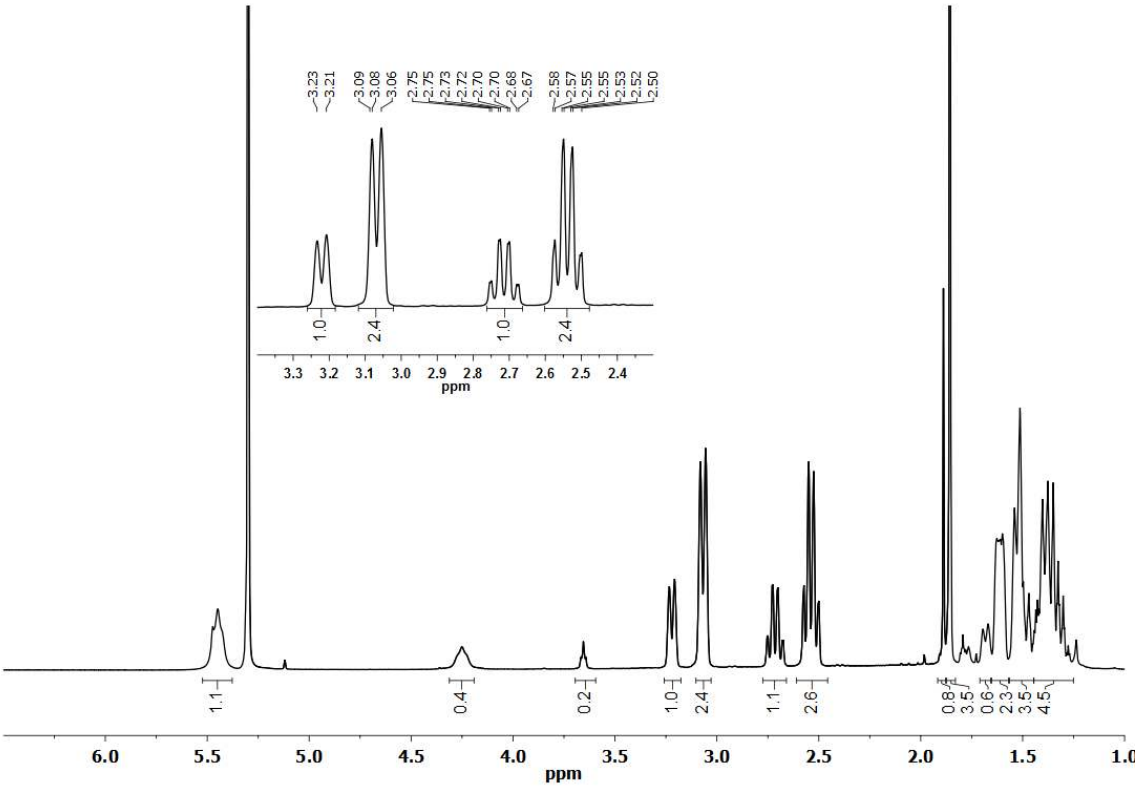

Figure 3: ^{1}H NMR spectrum of the mixture obtained from the reaction of impure $Pd(OAc)_2$ with piperidine {$Pd(OAc)(NO_2)(pip)_2$ and $Pd(OAc)_2(pip)_2$} in $CDCl_3$ (400 MHz).

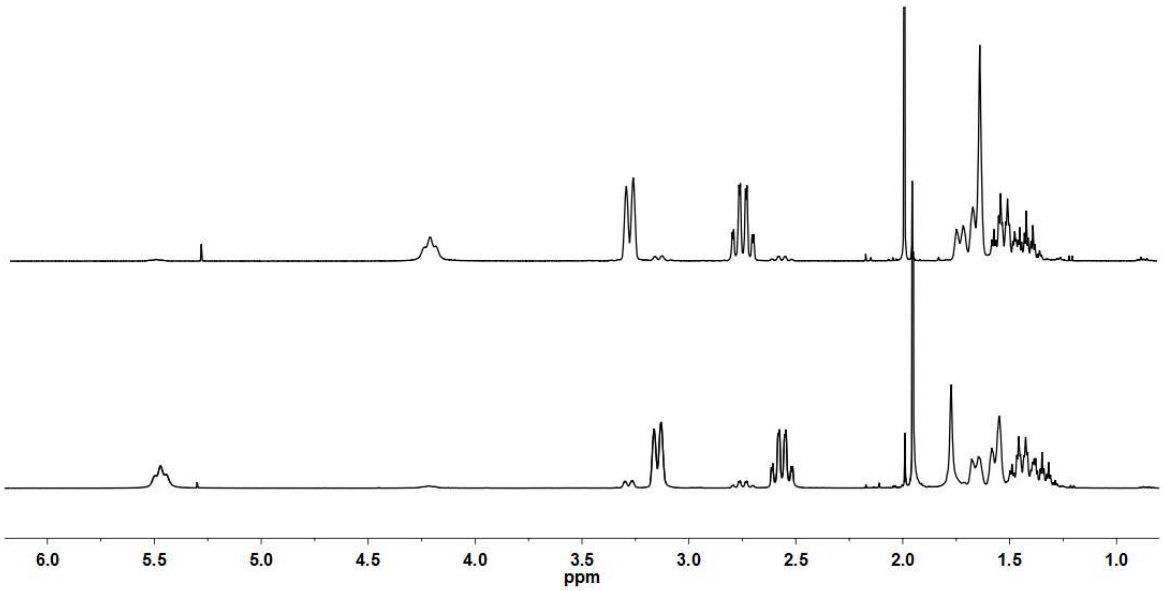

Figure 4: ^{1}H NMR overlay spectra of $Pd(OAc)(NO_2)(pip)_2$ (top) and $Pd(OAc)_2(pip)_2$ (bottom) in $CDCl_3$ (400 MHz).

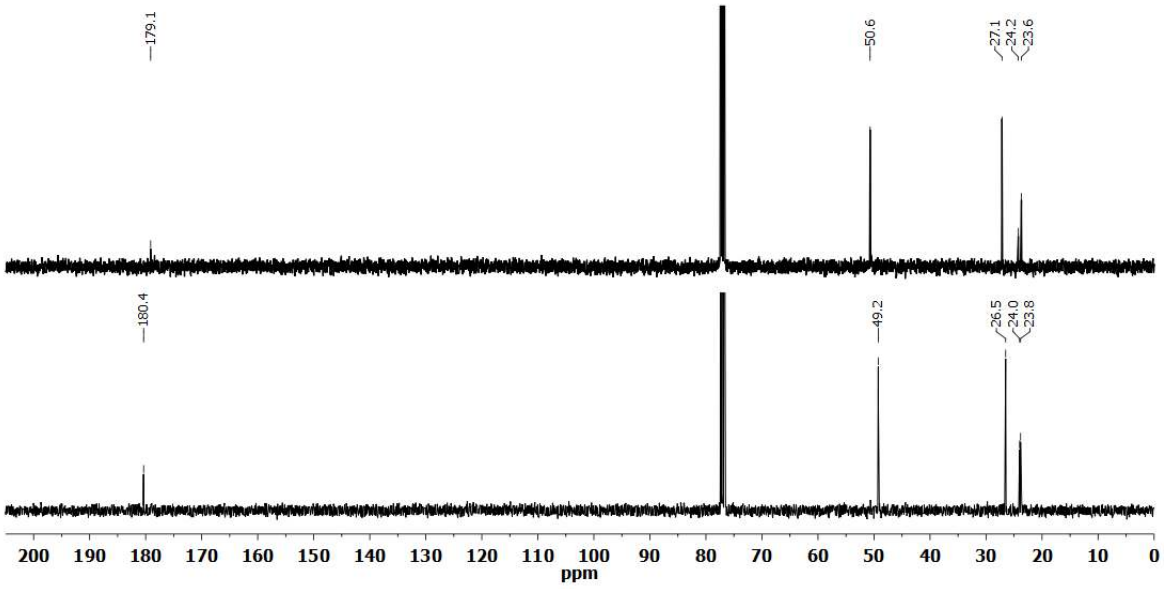

Figure 5: ^{13}C NMR overlay spectra of $Pd(OAc)(NO_2)(pip)_2$ (top) and $Pd(OAc)_2(pip)_2$ (bottom) in $CDCl_3$ (101 MHz).

4. Catalytic evaluation of $Pd(OAc)(NO_2)(pip)_2$ and $Pd(OAc)_2(pip)_2$

4.1. Direct arylation of 2'-deoxyadenosine

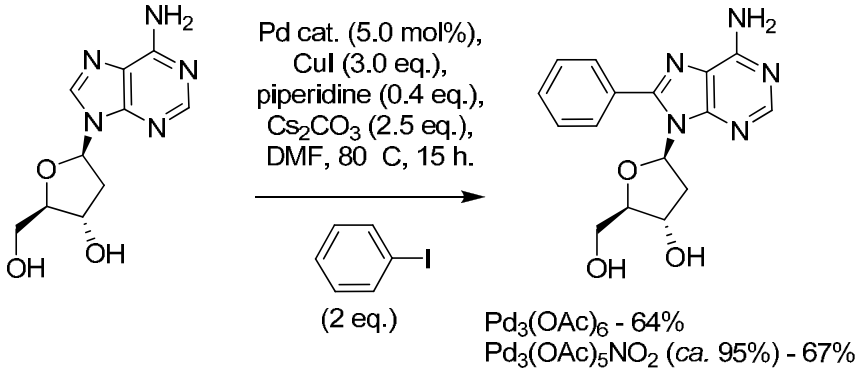

To a vacuum-dried Schlenk tube was added 2'-deoxyadenosine (473 mg, 1.88 mmol, 1.0 eq.), CuI (1.07 g, 5.61 mmol, 3.0 eq.), $Pd_3(OAc)_5(NO_2)$ (95% purity; 21 mg, 31 µmol, 1.7 mol%), Cs_2CO_3 (1.53 g, 4.68 mmol, 2.5 eq.), and iodobenzene (410 µl, 3.74 mmol, 2.0 eq.). The reaction vessel was evacuated under high vacuum at room temperature with stirring, then flushed with N_2 (three cycles). 'Extra dry' DMF (10 ml) from Acros was then added along with degassed piperidine (stored over 3Å molecular sieves, 74 µl, 0.75 mmol, 0.4 eq.). The vessel was then sealed and then heated in an oil bath at 80 °C and stirred continuously for 15 hours. The mixture was allowed to cool to ambient temperature, and 1M HCl solution (10 mL) added. The pH was then adjusted to 6.5 with 1M NaOH and the aqueous solution extracted with ^{i}PrOH:EtOAc (1:9, v/v, 5x50 mL), by decanting from the reaction mixture. The organic extracts were combined, dried ($MgSO_4$), filtered and reduced *in vacuo* to yield a thick gum, which was dried under high vacuum (ca. 0.8 mmHg). The

crude mixture was re-dissolved/suspended in MeOH:CH_2Cl_2 (1:1 v/v, 20 mL) and adsorbed onto silica gel (approximately 0.5 g), with reduction *in vacuo*. A short silica gel column (approximately 10 g) was eluted using MeOH:CH_2Cl_2 (2:98 v/v, moving in stepwise increments to 10:90 by gradient elution). The fractions containing the product were combined and the solvents removed *in vacuo*, then CH_2Cl_2 (10 mL) added and then removed (to remove residual MeOH), which gave the product as a light brown solid (412 mg, 67%). The characterisation data is identical to that reported in the literature.[3] Mp 124-126 ºC (decomp.); RP HPLC (monitoring at 254 nm), tR = 18.6 min, peak area = 96 %; UV-Vis, λ_{max} 280 nm; ^{1}H NMR (400 MHz, DMSO-d_6) δ 8.15 (s, 1H), 7.70 (m, 2H), 7.59 (m, 3H), 7.46 (brs, 2H), 6.15 (dd, *J* = 8.7, 6.2 Hz, 1H), 5.58 (dd, *J* = 8.3, 4.0 Hz, 1H), 5.24 (d, *J* = 4.0 Hz, 1H), 4.45 (ap.ddt, *J* = 5.8, 4.0, 1.9 Hz, 1H), 3.87 (ap.td, *J* = 4.2, 1.9 Hz, 1H), 3.69 (ddd, *J* = 12.2, 4.2, 4.0 Hz, 1H), 3.53 (ddd, *J* = 12.2, 8.3, 4.2 Hz, 1H), 3.30 (ddd, *J* = 13.2, 8.7, 5.8 Hz, 1H), 2.15 (ddd, *J* = 13.2, 6.2, 1.9 Hz, 1H); ^{13}C NMR (101 MHz, DMSO-d_6) δ 156.1, 152.0, 150.4, 149.8, 130.1, 129.6, 129.4, 128.8, 119.1, 88.4, 85.7, 71.4, 62.3, 37.2; ESI MS, *m/z* 328 [8.1 % $(M + H)^+$], 212 [100 % $(M - \beta D\text{-Ribose} + 2H)^+$]; HRMS (MH^+) 328.1394 (Calcd. for $C_{16}H_{18}O_3N_5$ 328.1404).

4.2. C2-Arylation of 1-methylindole[4]

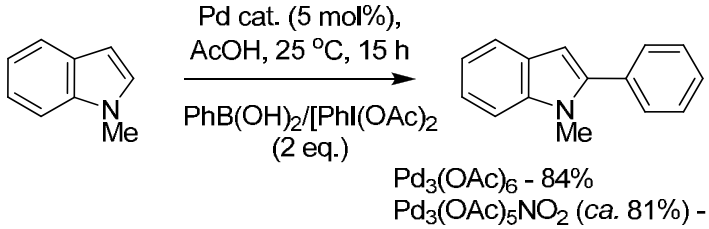

Using pure $Pd(OAc)_2$ (>99%): In a microwave reactor (thick-walled glass) tube under air, diacetoxyiodobenzene (246 mg, 0.763 mmol, 2.0 eq.), phenyl boronic acid (93 mg, 0.763 mmol, 2.0 eq.) and $Pd(OAc)_2$ (4 mg, 0.018 mmol) were dissolved in acetic acid (5 mL). The reaction mixture was stirred at 40 °C for ten minutes to give a dark orange solution. 1-Methylindole (50 mg, 48 µL, 0.381 mmol, 2.0 eq.) was added and the reaction mixture stirred at 40 °C for fifteen hours. During the course of this period, a black precipitate formed. The mixture was cooled to room temperature, filtered through a pad of Celite®, and the solvent removed *in vacuo*. The resulting brown solid was redissolved in ethyl acetate (20 mL) and washed with a saturated aqueous solution of $NaHCO_3$ (20 mL). The organic layer was collected, dried ($MgSO_4$), filtered and the solvent removed *in vacuo*. The resulting solid was purified by silica column chromatography (eluting with 4% ethyl acetate in petroleum ether 40-60 ºC) to give a white solid (67 mg, 84% yield). Mp 101-103 °C (Lit. 99-102 °C); ^{1}H NMR (500 MHz, $CDCl_3$) δ 7.65 (dt, *J* = 8.1, 1.0 Hz, 1H), 7.55-7.51 (m, 2H), 7.48 (t, *J* = 7.5 Hz, 2H), 7.43-7.39 (m, 1H), 7.38 (dd, *J* = 8.1, 1.0 Hz, 1H), 7.26 (ddd, *J* = 8.1, 7.0, 1.0 Hz, 1H), 7.16 (ddd, *J* = 8.1, 7.0, 1.0 Hz, 1H), 6.58 (s, 1H), 3.76 (s, 3H); ^{13}C NMR (126 MHz, $CDCl_3$) δ 141.6, 138.4, 132.9, 129.4, 128.5, 128.0, 127.8, 121.6, 120.5, 119.8, 109.6,

101.7, 31.1; ESI-MS *m/z* 208 ($[M+H]^+$); HRMS *m/z* 208.1120 ($[M+H]^+$) (calc. for $C_{15}H_{14}N$ 208.1121); IR ($CDCl_3$ solution, cm^{-1}) ν 3061, 2948, 2365, 2338, 2245, 1470; UV-Vis (cyclohexane, nm)[5] λ_{max} 206 (26304), 222 (ε = 27028 mol dm^{-3} cm^{-1}), 298 (ε = 15334 mol dm^{-3} cm^{-1}).

Using *ca.* 81% $Pd_3(OAc)_5NO_2$: An identical procedure was used as above, using $Pd_3(OAc)_5NO_2$ as the catalyst/precatalyst, which gave the product as a white solid (67 mg, 84% yield).

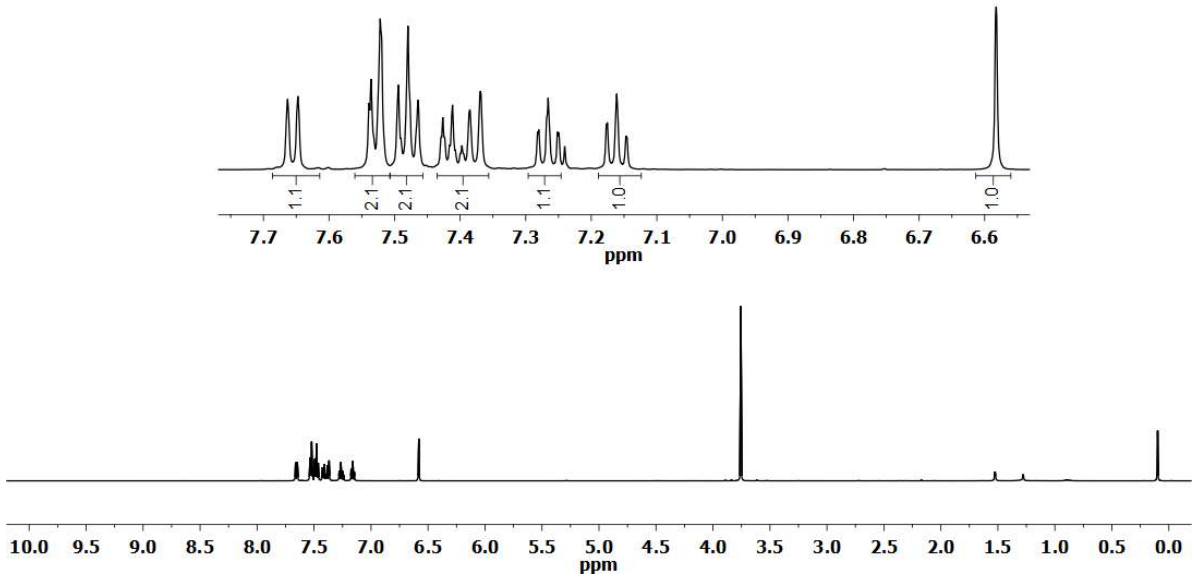

Figure 6: ^1H NMR spectrum of 2-phenyl-1-methylindole (400 MHz, $CDCl_3$).

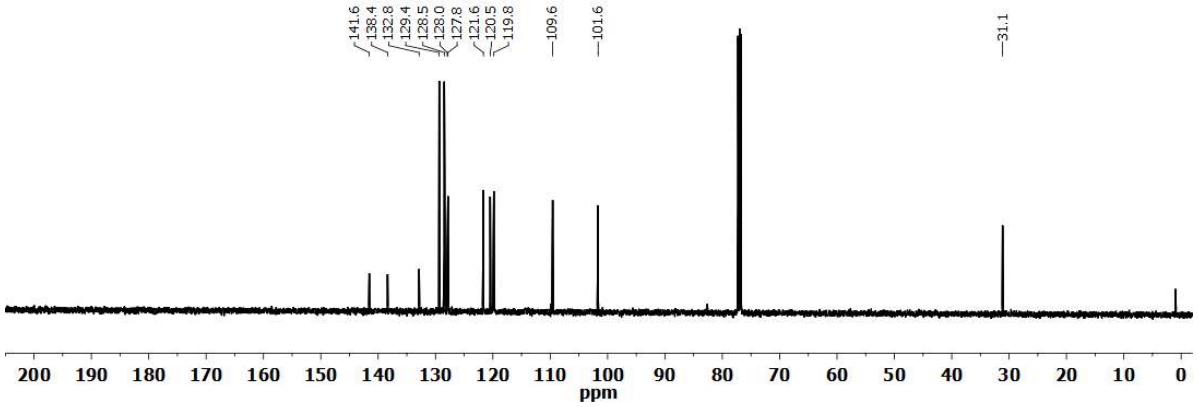

Figure 7: ^{13}C NMR spectra of 2-phenyl-1-methylindole (101 MHz, $CDCl_3$).

5. Palladation of papaverine (Hpap)

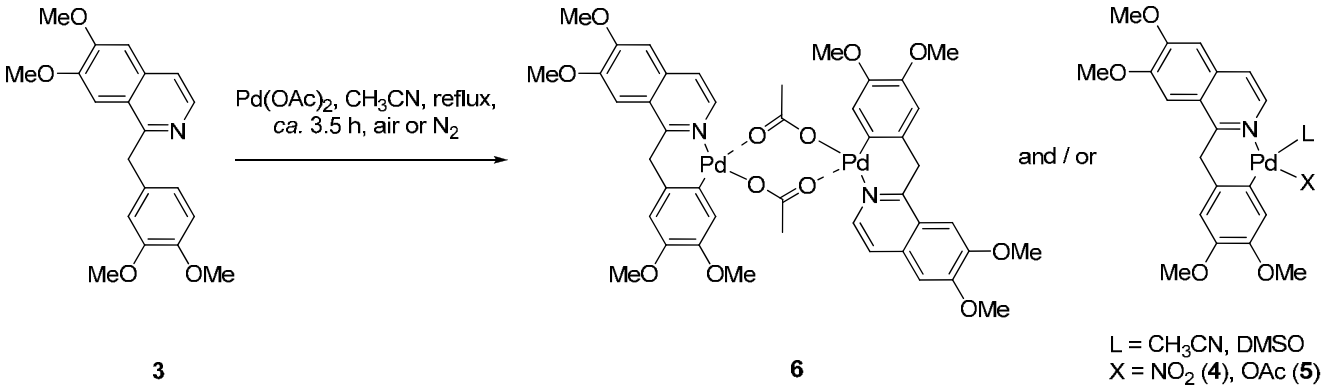

3 6

5.1. Reactions of Hpap (3) with $Pd(OAc)_2$ (>99%)

5.1.1. In air using reagent grade CH_3CN

A mixture of $Pd(OAc)_2$ (224 mg, 1 mmol) and commercially available Hpap (339 mg, 1 mmol; also available as the HCl salt – which can be removed on Amberlite^{TM} eluting with CH_2Cl_2) in acetonitrile (30 mL) was refluxed for 3.5 h (under air atmosphere) with stirring. The resultant dark coloured solution was filtered whilst hot to remove metallic palladium formed during the reaction. The filtrate was then kept in the fridge which led to yellow crystals being formed. After 14 days, the yellow semi-crystalline material was filtered, washed with hexane and dried *in vacuo* to give **6** (0.415 g, 82%). The characterisation data for the material produced from this reaction is given in section 5.1.4.

5.1.2. In air using triply-distilled CH_3CN

Procedure identical to that reported in 5.1.1. After 14 days, the yellow semi-crystalline material was filtered, washed with hexane and dried *in vacuo* to give **6** (0.225 g, 44%). The characterisation data for the material produced from this reaction is given in section 5.1.4.

5.1.3. Under N_2 atmosphere using triply-distilled CH_3CN

Procedure identical to that reported in 5.1.1, with the exception that the reaction was conducted under N_2 (Schlenk techniques). After 14 days, the yellow semi-crystalline material was filtered, washed with hexane and dried *in vacuo* to give **6** (0.339 g, 67%). The characterisation data for the material produced from this reaction is given in section 5.1.4.

Note: the yields quoted above (in 5.1.1.-5.1.3.) reflect the efficiency of the crystallisation step and not (necessarily) reaction efficacy. In all cases, ^{1}H NMR spectroscopic analysis of the crude reaction mixture(s) indicated that cyclopalladation had fully occured within less than one hour).

5.1.4. Characterisation data for complex 6

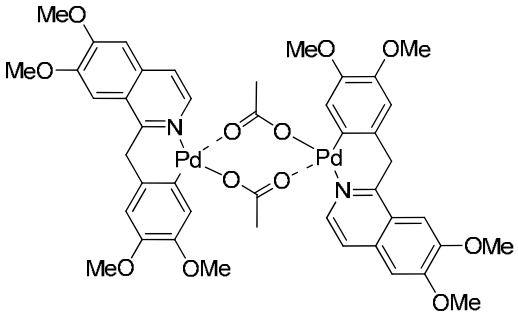

In both DMSO-d_6 and CD_3CN a mixture of compounds (tentatively assigned as either mononuclear and/or isomeric dinuclear complexes) were observed by ^{1}H NMR spectroscopy. A typical NMR spectrum in DMSO-d_6 is shown in section 5.1.4.1.

5.1.4.1 NMR spectroscopic data for complex 6

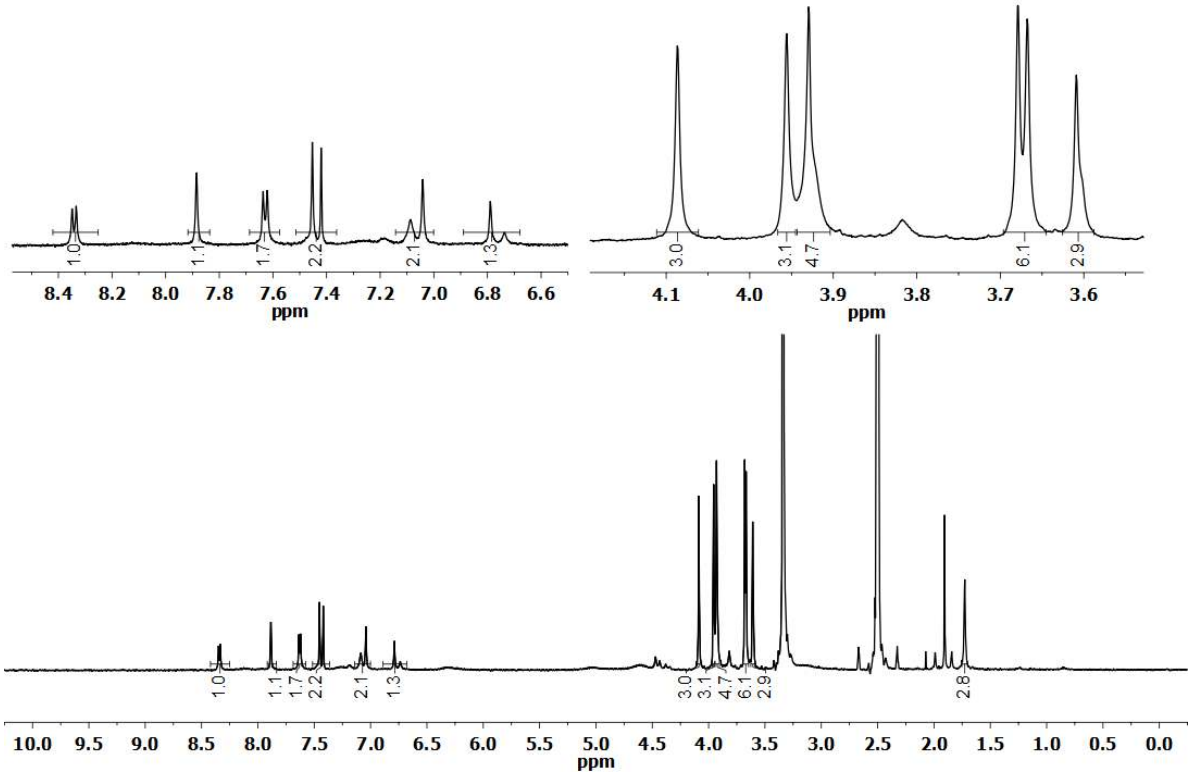

Figure 8: ^{1}H NMR spectra of complex **6** in DMSO-d_6 (400 MHz).

Dissolution of the same material in pyridine-d_5 {residual peaks at δ 8.74, 7.59, 7.22 and 5.04 (H_2O)} gave the following ^{1}H NMR spectrum:

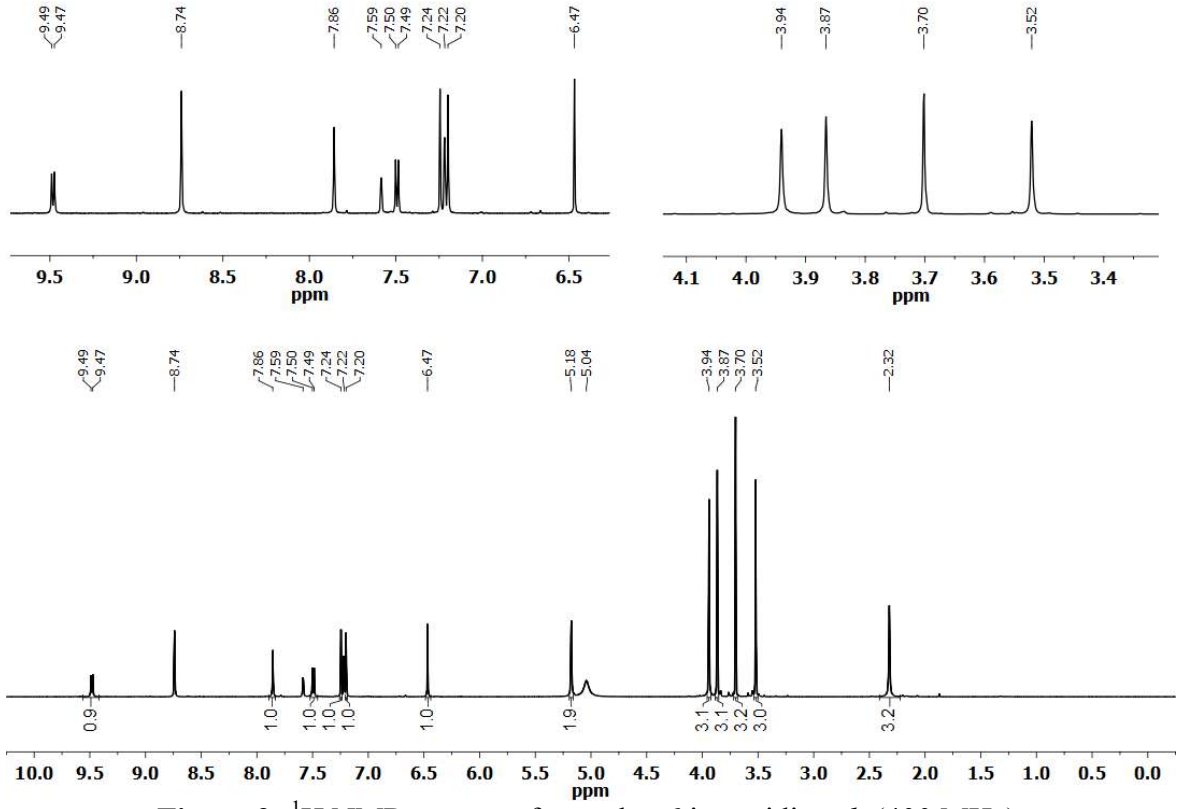

Figure 9: ^{1}H NMR spectra of complex **6** in pyridine-d_5 (400 MHz).

Irrespective of the reaction conditions used (air or N_2 atmosphere) the same ^{1}H NMR spectrum is recorded (as shown above in Fig. 9) in pyridine-d_5. The following structure is therefore proposed:

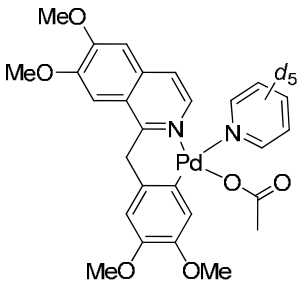

^{1}H NMR (400 MHz, pyr-d_5) δ 9.48 (d, J = 6.5 Hz, 1H), 7.86 (s, 1H), 7.49 (d, J = 6.5 Hz, 1H), 7.24 (s, 1H), 7.20 (s, 1H), 6.47 (s, 1H), 5.18 (s, 2H), 3.94 (s, 3H), 3.87 (s, 3H), 3.70 (s, 3H), 3.52 (s, 3H) and 2.32 (s, 3H) (**note:** after 24 h in solution this complex does degrade to give other uncharacterised species).

5.1.4.2 Other characterisation data (DMSO adduct of 6)

Mp 225-226 (decomp.)°C; LIFDI MS *m/z* 503 ($[M]^{+\cdot}$), 337 (100); HR-MS *m/z* 503.0524 ($[M]^{+}$) (calc. for Pd($C_{22}H_{23}NO_6$ 503.0560) {**note:** a complex mixture of ions were observed at *m/z* 1002-1014 (dimer), but an accurate mass could not be determined}; IR (KBr) υ cm^{-1} 2938, 2835, 1618, 1575, 1511, 1484, 1465, 1423, 1274, 1254, 1239, 1207, 1159, 1043, 1027, 987, 857, 824, 781, 681; Elemental Analysis, Calcd. for

$C_{48}H_{58}N_2O_{14}Pd_2S_2$ (**6**·2DMSO) (found) %: C 49.53 (48.98), H 5.02 (4.82), N 2.41 (2.37) (**note:** elemental analysis on crystalline material derived from DMSO).

5.2. Reactions of Hpap with impure $Pd(OAc)_2$ {mixture of $Pd_3(OAc)_6$ and $Pd_3(OAc)_5NO_2$}

5.2.1. In air using triply-distilled CH_3CN

Procedure (and scale) identical to that reported in 4.1.1 using impure $Pd_3(OAc)_6$ {*ca.* 81% $Pd_3(OAc)_5NO_2$}. After 14 days, the yellow semi-crystalline material was filtered, washed with hexane and dried *in vacuo* to give a mixture of compounds (0.137 g, *ca.* 27%); Whilst the ^{1}H NMR spectrum of this material is quite complicated (see below), MS analysis reveals only the presence of a [Pd(C^N)(OAc)] adduct – LIFDI MS *m/z* 503.06 ($[M]^{+\cdot}$); Elemental analysis of this material, Found: C, 48.73; H, 4.45; N, 4.20 (high nitrogen content).

5.2.1.1. ^{1}H NMR spectrum (in DMSO-d_6, 400 MHz)

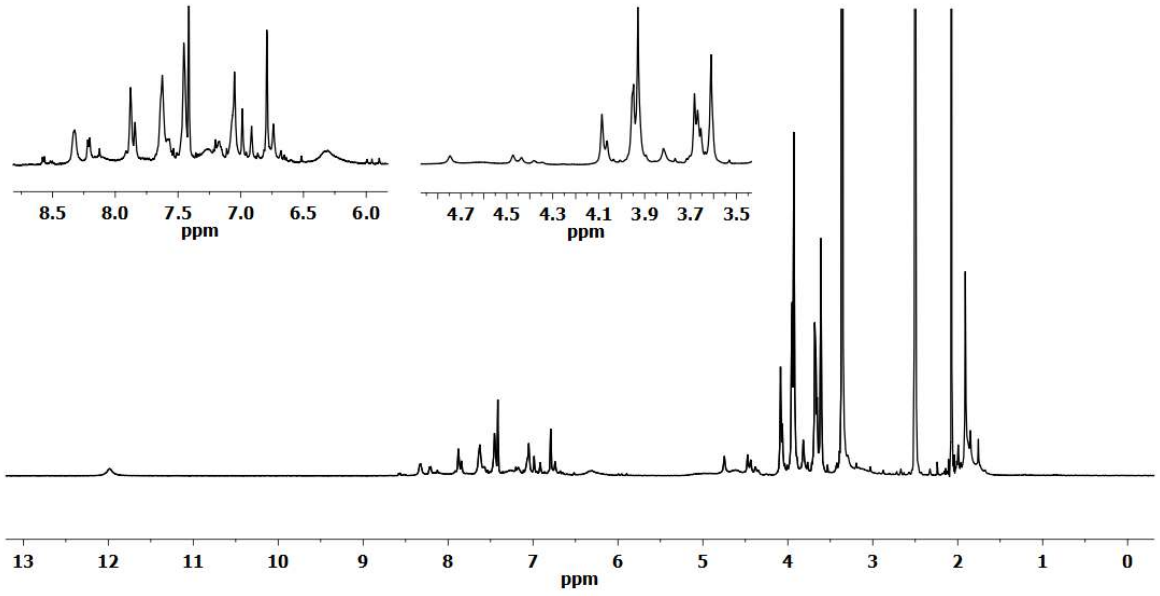

Figure 10: ^{1}H NMR spectrum of material produced from the reaction of papaverine with impure $Pd(OAc)_2$ in air using triply-distilled CH_3CN. **Note:** the proton signals have not been intergrated (this spectrum is for illustrative purposes only). Also, note the presence of acetic acid (*ca.* δ 12.0 ppm).

5.2.2. Under N_2 atmosphere using triply-distilled CH_3CN

Procedure (and scale) identical to that reported in 4.1.1 using impure $Pd_3(OAc)_6$ {*ca.* 81% $Pd_3(OAc)_5NO_2$}. After 14 days, the yellow semi-crystalline material was filtered, washed with hexane and dried *in vacuo* to give a mixture of compounds (0.175 g, *ca.* 35 %); Whilst the ^{1}H NMR spectrum of this material is quite complicated (see below), MS analysis reveals only the presence of a [Pd(pap)(OAc)] adduct – LIFDI MS *m/z* 503.01 ($[M]^{+\cdot}$), 339.12 (100); Elemental analysis of this material, Found: C, 47.9; H, 4.64; N, 8.62 (high nitrogen content).

5.2.2.1. ^{1}H NMR spectrum (in DMSO-d_6, 400 MHz)

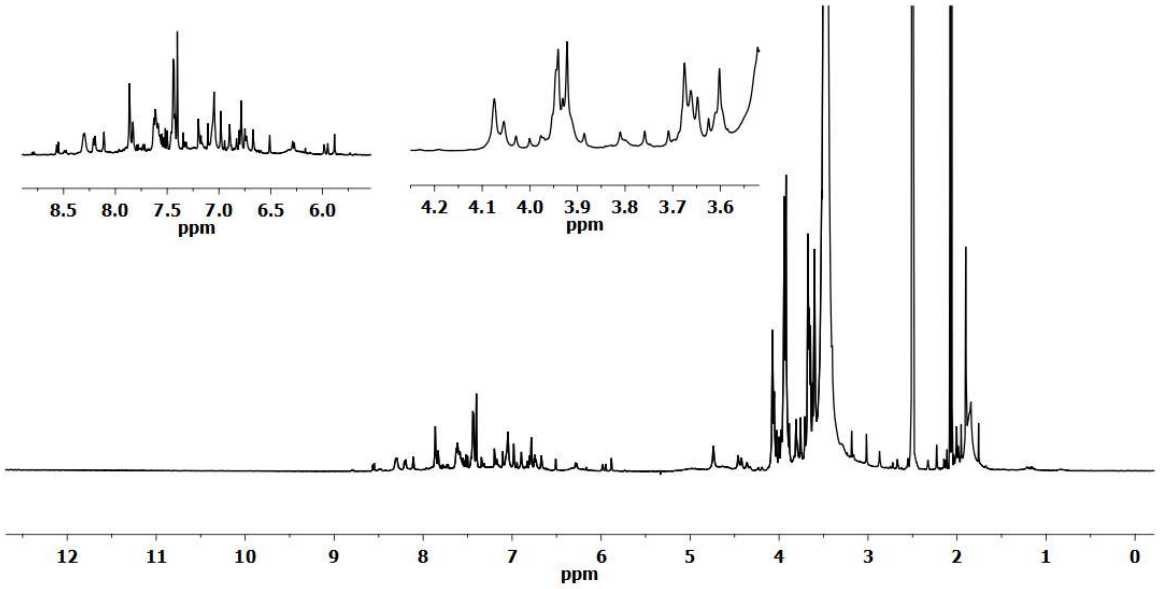

Figure 11: ^{1}H NMR spectrum of material produced from the reaction of papaverine with impure $Pd(OAc)_2$ under nitrogen, using triply-distilled CH_3CN. **Note:** the proton signals have not been intergrated (this spectrum is for illustrative purposes only).

5.3. Synthesis of [Pd(OAc)(C^N)PPh$_3$]: Reaction of 6 with PPh$_3$

Palladium complex **6** (150 mg, 7.5x10^{-5} mol) was dissolved in dichloromethane (15 mL) containing triphenylphosphine (78.1 mg, 0.15 mmol, 1 eq. per Pd) was added. The solution was refluxed at 40 ºC for 2 h, and then concentrated *in vacuo* to one fifth of its initial volume. Slow addition of diethyl ether led to precipitation of the complex, which was filtered off, washed with diethyl ether and air-dried to afford a pale yellow solid (0.089 g, 39%). Mp 135-137 (decomp.); ^{1}H NMR (400 MHz, CD_2Cl_2) δ 8.53 (d, J = 6.3 Hz, 1H), 7.55-7.66 (br m, 7H), 7.41-7.45 (br m, 3H), 7.34-7.39 (br m, 7H), 7.03 (s, 1H), 6.81 (s, 1H), 6.04 (d, J = 4.5 Hz, 1H), 4.96 (br d, *ca.* 12 Hz, 1H), 4.82 (br d, *ca.* 12 Hz, 1H), 4.09 (s, 3H), 3.97 (s, 3H), 3.69 (s, 3H), 2.91 (s, 3H), 1.21 (s, 3H); ^{13}C NMR (101 MHz, CD_2Cl_2) δ 177.3 (4º), 158.3 (4º), 154.8 (4º), 151.5 (4º), 146.3 (4º, d, J = 2.5 Hz), 146.1 (4º), 142.8 (CH), 135.5 (CH, d, J = 11.5 Hz), 134.5 (4º), 131.5 (4º, d, J = 48 Hz), 131.1 (4º), 130.9 (CH, d, J = 1.5 Hz), 128.8 (CH, d, J = 10.5 Hz), 122.9 (4º, d, J = 2.5 Hz), 119.9 (CH, d, J = 11 Hz), 119.2 (CH), 112.8 (CH), 105.9 (CH), 104.6 (CH), 56.7 (CH_3), 56.6 (CH_3, 2C), 55.1 (CH_3), 45.1 (CH_2), 24.1 (CH_3); ^{31}P NMR (162 MHz, CD_2Cl_2) δ 34.6 (s, 1P); IR (KBr) υ cm^{-1} 2935, 2834, 1619, 1575, 1510, 1483, 1464, 1422, 1337, 1312, 1274, 1238, 1207, 1160, 1096, 1042, 987; LIFDI MS *m/z* 765 $[M]^{+\cdot}$, 503 (100), HR-MS *m/z* 765.1260 ($[M+H]^+$) (calc. for $C_{40}H_{38}NO_6PdP$ 766.1312).

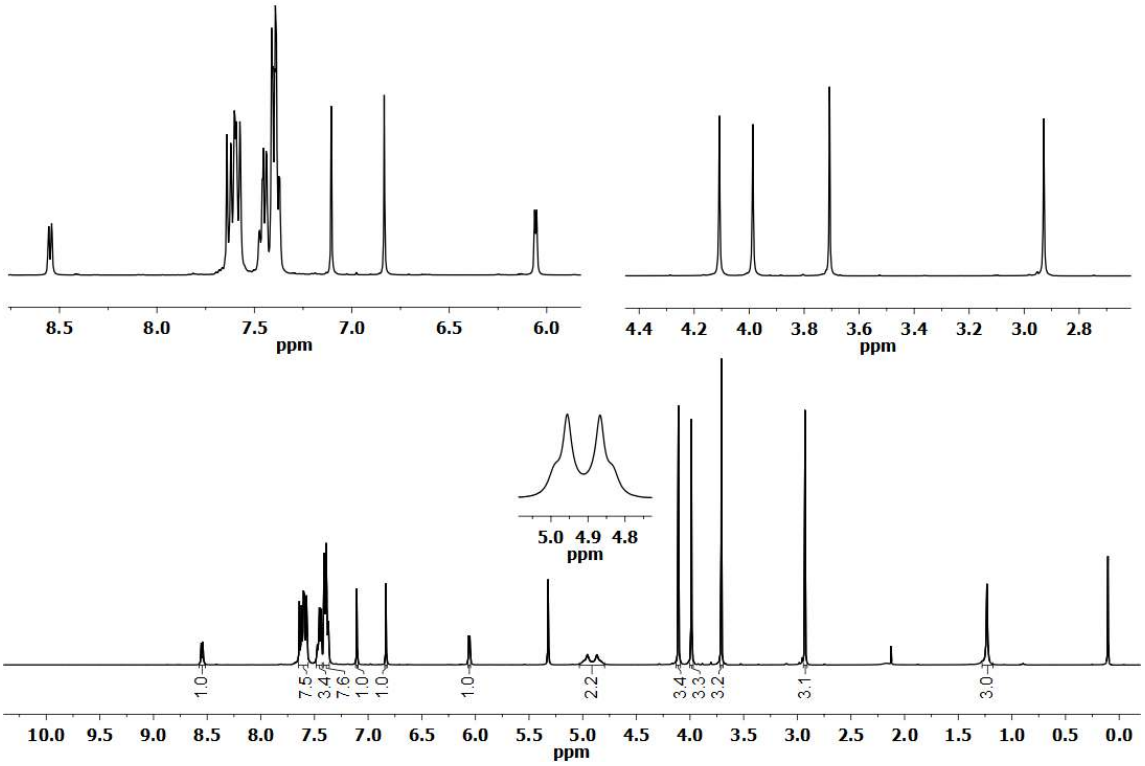

Figure 12: ^{1}H NMR spectrum of [Pd(OAc)(C^N)PPh$_3$] in CD_2Cl_2 (400 MHz).

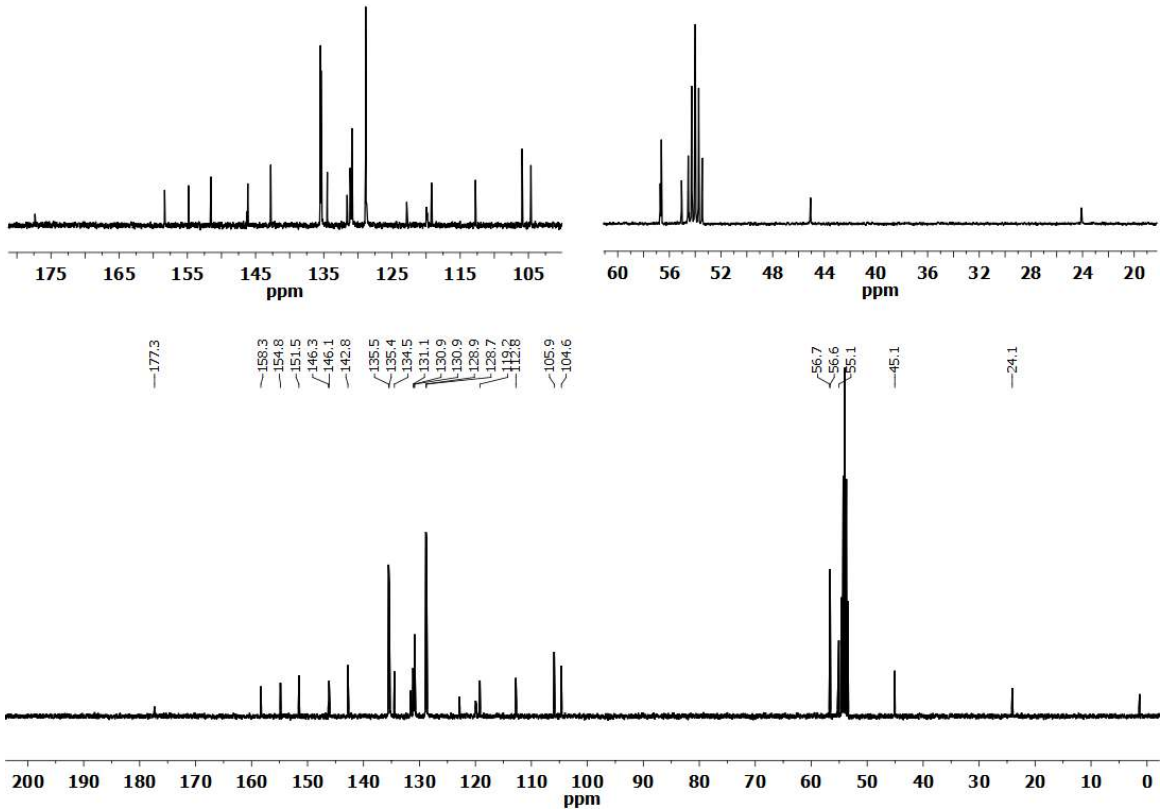

Figure 13: ^{13}C NMR spectrum of [Pd(OAc)(C^N)PPh$_3$] in CD_2Cl_2 (101 MHz).

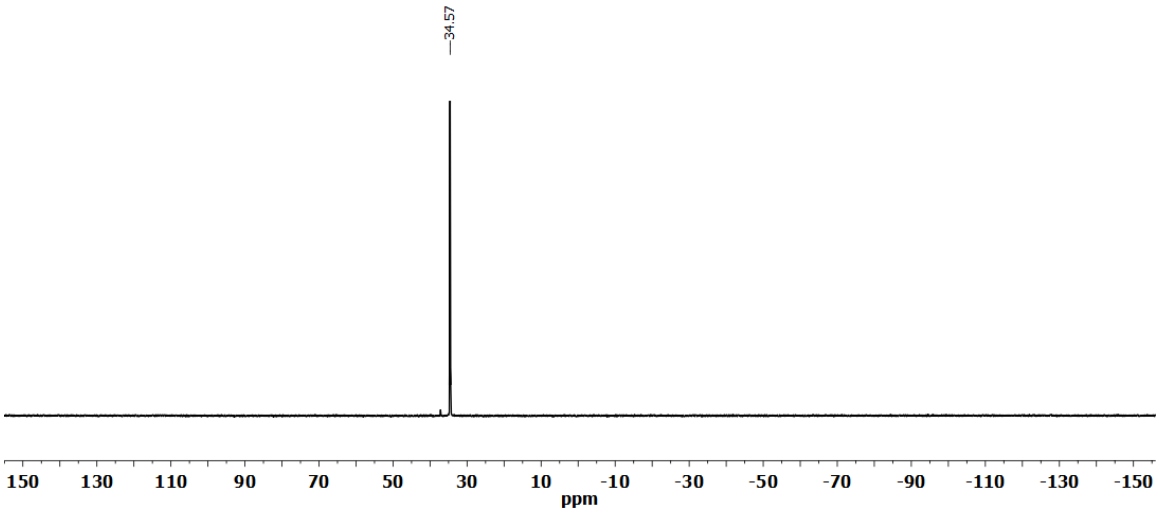

Figure 14: ^{31}P NMR spectrum of [Pd(OAc)(C^N)PPh$_3$] in CD_2Cl_2 (162 MHz).

5.4. Synthesis of an authentic sample of [Pd(NO$_2$)(C^N)CH$_3$CN]·1.5H$_2$O: Reaction of 6·CH$_3$CN with NaNO$_2$

To a stirred solution of $NaNO_2$ (73.8 mg, 1.07 mmol, 10 eq.) in CH_3CN (10 mL) was added semi-crystalline **6**·CH_3CN (0.112 g, 0.107 mmol, 1 eq.). The mixture was refluxed for 2 h (temperature *ca.* 90 ºC, solution turned from yellow to green), and then filtered through dried Celite® whilst hot to remove any insoluble material (trace palladium black and insoluble $NaNO_2$/NaOAc). The title complex precipitated out of solution overnight (left open to air), which was filtered and washed with diethyl ether and then dried *in vacuo* affording a pale yellow solid (78.0 mg, 69%). Mp 204-206 (dec.); ^{1}H NMR (400 MHz, DMSO-d_6) δ 8.23 (br s, 1H, H-3), 7.85 (s, 1H, H-8), 7.58 (br s, 1H, H-4,), 7.44 (s, 1H, H-5), 6.98 (s, 1H, H-5`), 6.91 (s, 1H, H-6`), 4.74 (br s, 2H, CH_2), 4.07 (s, 3H, OCH_3), 3.95 (s, 3H, OCH_3), 3.65 (s, 3H, OCH_3), 3.61 (s, 3H, OCH_3), 2.07 (s, 2H, liberated CH_3CN); ^{13}C NMR (101 MHz, DMSO-d_6, note: weak spectrum – an improved spectrum was recorded in CD_2Cl_2, see below) δ 158.7, 154.1, 150.9, 146.0, 144.9, 141.4, 133.3, 122.0, 118.1, 111.9, 105.8, 104.9, 56.4, 56.1, 56.0, 55.6, 48.6, 30.7, 1.2 (liberated CH_3CN); ^{13}C NMR (101 MHz, CD_2Cl_2) δ 159.0, 155.5, 152.1, 147.4, 146.3, 142.2, 134.6, 128.4, 123.2, 119.8, 117.2, 111.9, 105.8, 104.6, 56.9, 56.8, 56.7, 55.7 44.3; IR (KBr) υ cm^{-1} 2970, 2839, 2283, 1619, 1564, 1512, 1484, 1462, 1451, 1424, 1378, 1336, 1273, 1237, 1207, 1160, 1043, 988; LIFDI MS *m/z* 490.05 [M-CH_3CN]$^{+\cdot}$, 339.15 (100); Elemental Analysis, Calcd. for Pd($C_{22}H_{26}N_3O_{7.5}$) (found) %: C 47.28 (47.42), H 4.69 (4.35), N 7.52 (7.86) (**note:** the complex is mononuclear and assigned as [Pd(NO_2)(C^N)CH_3CN]·1.5H_2O). Following repeated attempts of this reaction (including varying the $NaNO_2$ equivalents to 10), in one case a single crystal of Pd(*N*-Hpap)$_2$(NO_2)$_2$ was obtained (which is not representative of the bulk material), which was subsequently characterised by X-ray diffraction methods (see section 6).

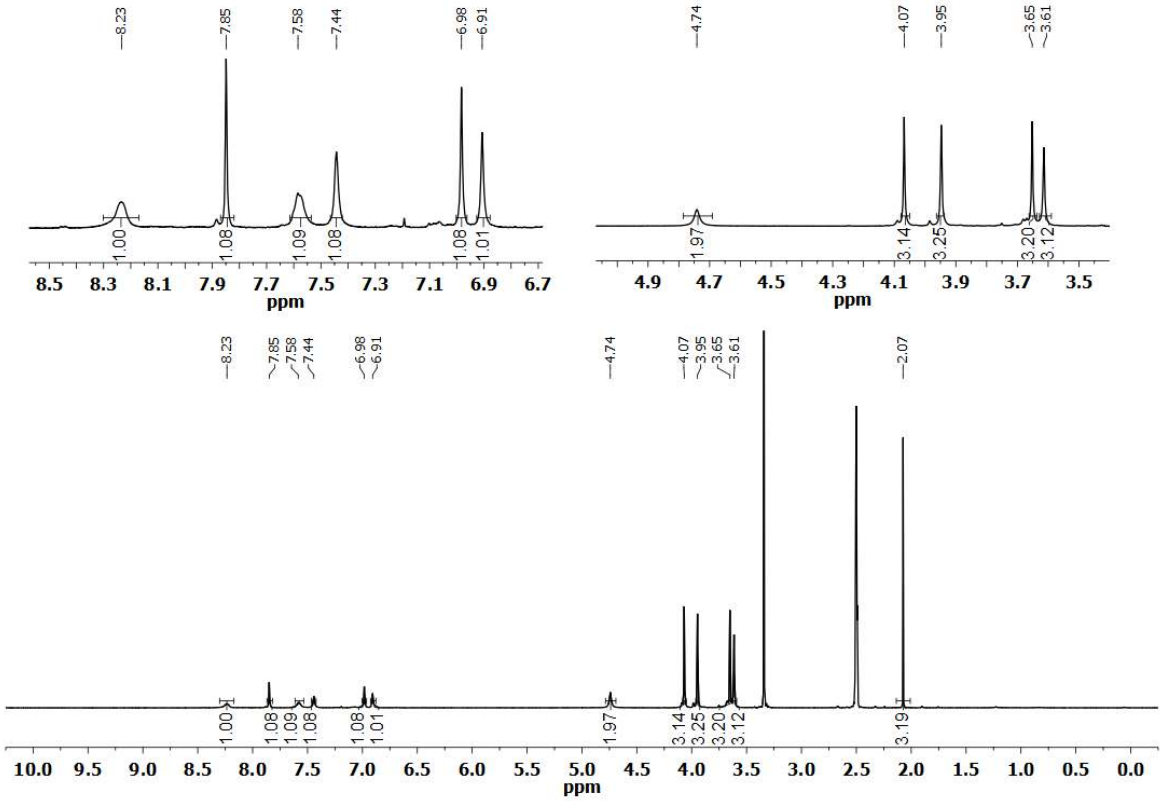

Figure 15: ^{1}H NMR spectrum of $[Pd(NO_2)(C^N)CH_3CN]\cdot 1.5H_2O$ in DMSO-d_6 (400 MHz). **Note:** the proton signal at δ 2.07 is liberated acetonitrile (1 eq. per Pd).

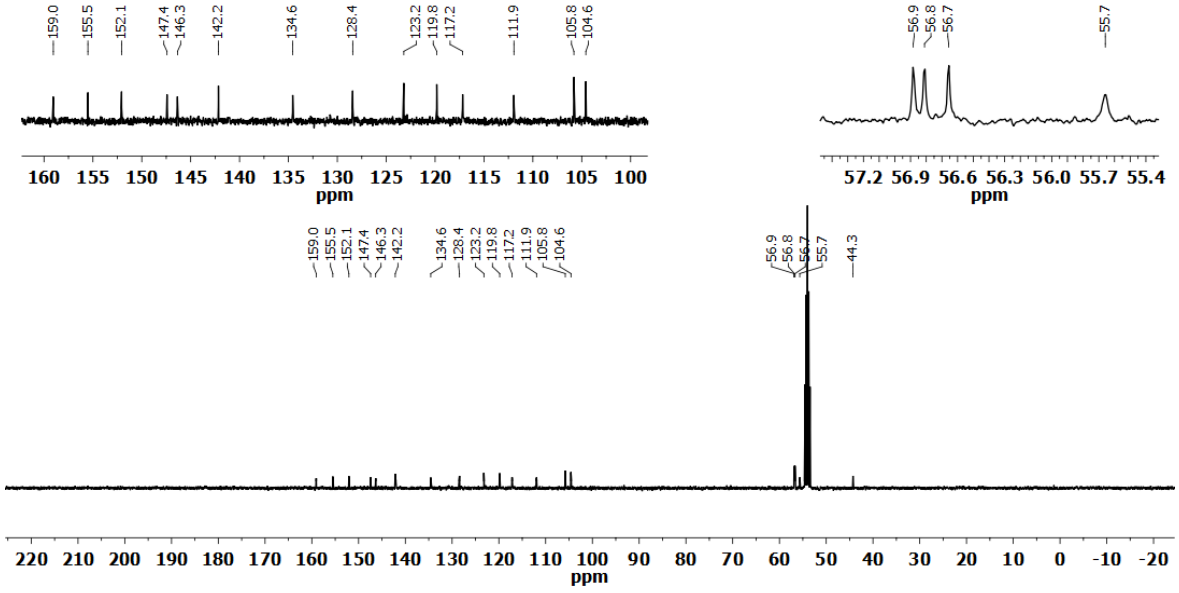

Figure 16: ^{1}H NMR spectrum of $[Pd(NO_2)(C^N)CH_3CN]\cdot 1.5H_2O$ in CD_2Cl_2 (400 MHz).

5.5. Comparison of NMR spectroscopic data for complex 4·CH_3CN

Table 1.[a]

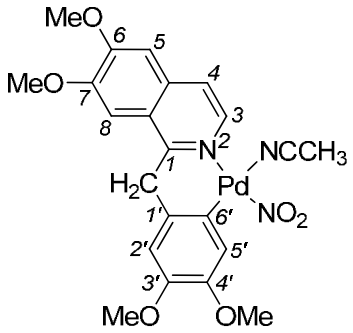

^{1}H signal	[Pd(NO_2)(C^N)CH_3CN]·3H_2O[b]	[Pd(NO_2)(C^N)CH_3CN]·1.5H_2O[c]
H-3	8.26 (d, *J* = 6.3)	8.23 (br s)
H-4	7.62 (d, *J* = 6.3)	7.58 (br s)
H-5,8	7.47 (s)	7.44 (s)
	7.88 (s)	7.85 (s)
H-5`,6`		-
	7.04 (s)	6.98 (s)
	6.96 (s)	6.91 (s)
CH_2	4.79 (s)	4.74 (br s)
OCH_3	4.11 (s)	4.07 (s)
	3.99 (s)	3.95 (s)
	3.70 (s)	3.65 (s)
	3.66 (s)	3.61 (s)

[a] Reported atom-numbering was used.
[b] Reported data for the palladium-nitrito adduct (in DMSO-d_6, 400 MHz).[6]
[c] in DMSO-d_6 at 400 MHz, 300 K.

5.6. Synthesis of [Pd(NO_2)(C^N)PPh_3]: Reaction of [Pd(NO_2)(C^N)CH_3CN]·1.5H_2O with PPh_3

Complex [Pd(NO_2)(C^N)CH_3CN]·1.5H_2O (0.035 g, 0.063 mmol) was dissolved in CH_2Cl_2 (10 mL). PPh_3 (16.4 mg, 0.063 mmol, 1 eq.) was then added. The solution was refluxed (40 ºC) for 2 h, and then concentrated *in vacuo* to one fifth of its initial volume. Addition of diethyl ether (5 mL) led to product precipitation, which was filtered, washed with diethyl ether (2 x 5 mL) and air-dried (32.3 mg, 68%; quantitative by ^{31}P NMR analysis of the reaction mixture). Mp 185-187 (decomp.); ^{1}H NMR (400 MHz, CD_2Cl_2) δ 8.24 (br d, *J ca.* 5 Hz, 1H), 7.63-7.56 (m, 7H), 7.50-7.45 (m, 3H), 7.41-7.34 (m, 7H), 7.09 (s, 1H), 6.77 (s, 1H), 6.01 (d, *J* = 4.7 Hz, 1H), 5.01 (d, *J* = 14.1Hz, 1H), 4.84 (d, *J* = 14.1 Hz, 1H), 4.10 (s, 3H), 3.98 (s, 3H), 3.68 (s, 3H), 2.98 (s, 3H); ^{13}C NMR (101 MHz, CD_2Cl_2) δ 158.6 (4º), 155.1 (4º), 151.8 (4º), 146.54 (4º), 146.46 (4º, d, *J* = 4.0 Hz), 141.9 (CH), 137.0 (4º), 135.2 (CH, d, *J* = 11.5 Hz), 134.7

(4º), 131.3 (CH, d, J = *ca.* 3 Hz), 131.0 (4º, d, J = *ca.* 45 Hz), 130.8 (4º), 129.0 (CH, d, J = 10.5 Hz), 123.2 (4º d, J = 3.5 Hz), 120.5 (CH, d, J = 12 Hz, 119.3 (CH, d, J = 2.5 Hz), 112.5 (CH), 106.0 (CH), 104.7 (CH), 56.73 (CH_3), 56.7 (2C, CH_3), 55.3 (CH_3), 45.1 (CH_2) {confirmed by DEPT135 experiment); ^{31}P NMR (162 MHz, CD_2Cl_2) δ (ppm): 32.7 (s, 1P); LIFDI MS *m/z* 706.22 $[C_{38}H_{35}NO_4PPd]^+$ (base peak); Elemental Analysis, Calcd. For $C_{38}H_{35}N_2O_6PdP{\cdot}1.25CH_2Cl_2$ (found) %: C 54.86 (54.37), H 4.40 (4.46), N 3.26 (3.35) (**note:** dichloromethane adduct).

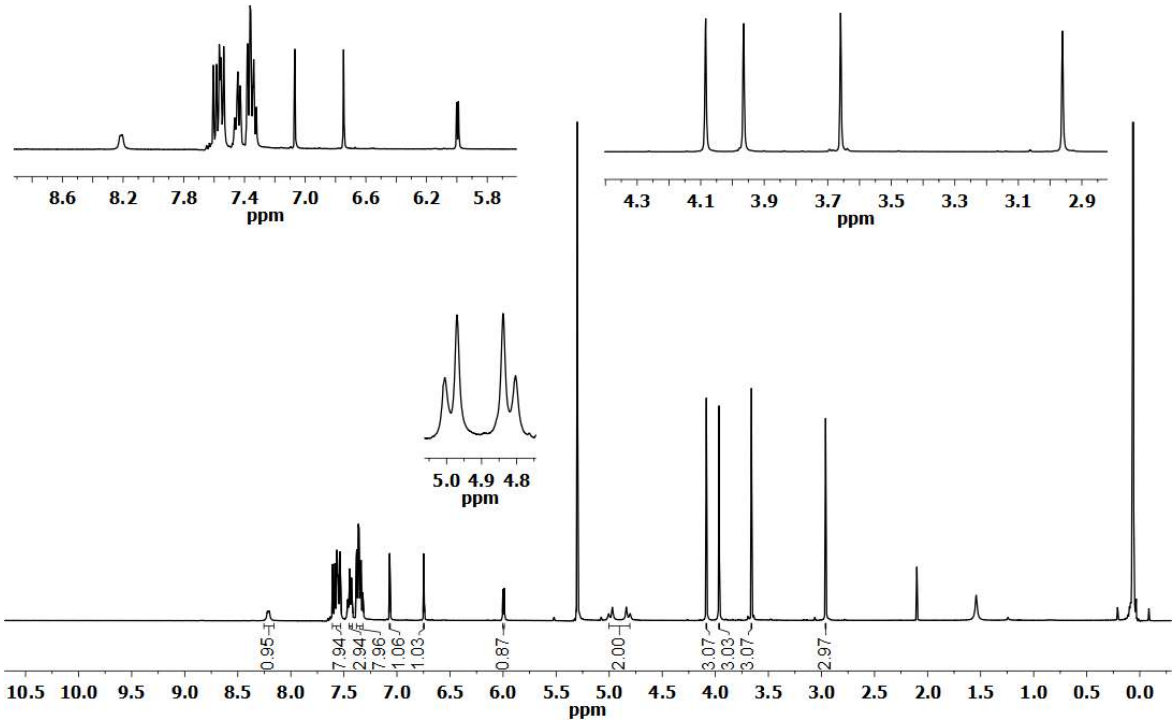

Figure 17: ^{1}H NMR spectrum of $[Pd(NO_2)(C\hat{}N)PPh_3]$ in CD_2Cl_2 (400 MHz).

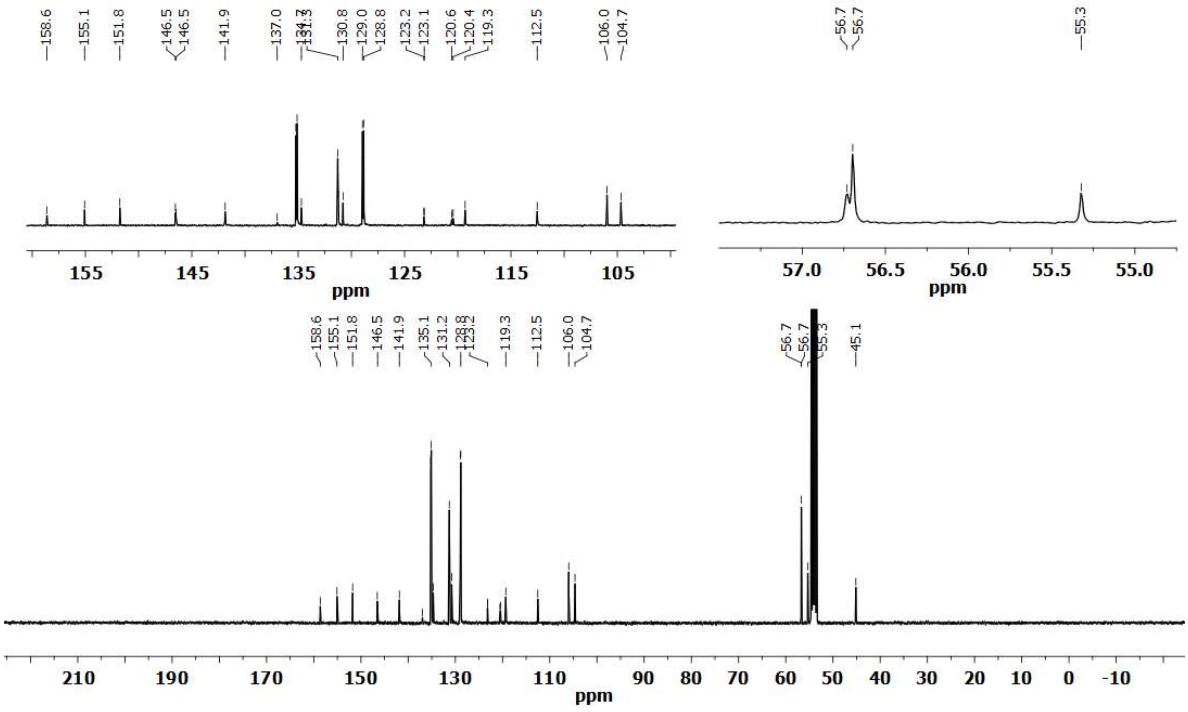

Figure 18: ^{13}C NMR spectrum of $[Pd(NO_2)(C\hat{}N)PPh_3]$ in CD_2Cl_2 (101 MHz).

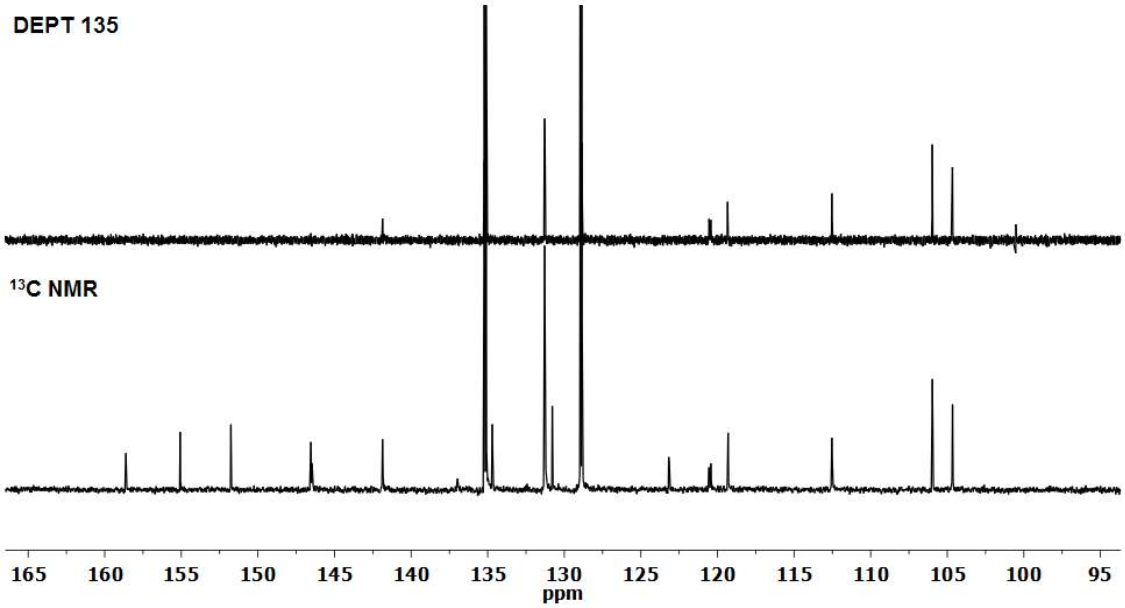

Figure 19: Overlay ^{13}C NMR / DEPT 135 spectra of $[Pd(NO_2)(C^N)PPh_3]$ in CD_2Cl_2 (101 MHz).

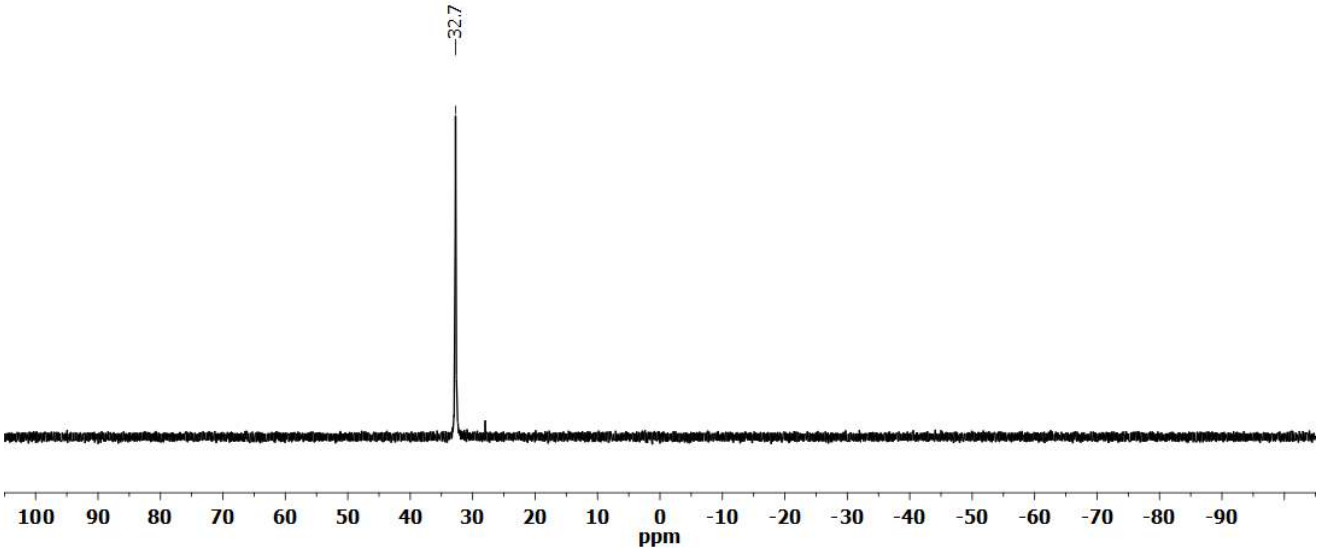

Figure 20: ^{31}P NMR spectrum of $[Pd(NO_2)(C^N)PPh_3]$ in CD_2Cl_2 (162 MHz).

6. X-ray crystallography

6.1. Crystallographic data for compounds analysed and solved in York

6.1.1. General details

Diffraction data for $Pd(OAc)_2(pip)_2$, $Pd(OAc)(NO_2)(pip)_2$, complex **6** and [Pd(OAc)(C^N)PPh_3] (**7**) were collected at 110 K on a Bruker Smart Apex diffractometer with Mo-K_α radiation (λ = 0.71073 Å) using a SMART CCD camera. Diffractometer control, data collection and initial unit cell determination was performed using "SMART".[7] Frame integration and unit-cell refinement was carried out with "SAINT+".[8] Absorption corrections were applied by SADABS.[9] Structures were solved by "direct methods" using SHELXS-97 (Sheldrick, 1997)[10] and refined by full-matrix least squares using SHELXL-97 (Sheldrick, 1997).[11] All non-hydrogen atoms were refined anisotropically. Hydrogen atoms were placed using a "riding model" and included in the refinement at calculated positions.

6.1.2. X-ray data for $Pd(OAc)_2(pip)_2$, $Pd(OAc)(NO_2)(pip)_2$, complex 6 and [Pd(OAc)(C^N)PPh_3] (7) and [Pd(*N*-Hpap)$_2$(NO_2)$_2$]

Table 2. X-data for complexes: $Pd(OAc)_2(pip)_2$, $Pd(OAc)(NO_2)(pip)_2$ and **6**.

Compound reference	ijf0915a [$Pd(OAc)_2(pip)_2$]	ijf0916m [$Pd(OAc)(NO_2)(pip)_2$}	ijf1020m (**6**)
Chemical formula	$C_{14}H_{28}N_2O_4Pd$	$C_{12}H_{25}N_3O_4Pd$	$C_{44}H_{46}N_2O_{12}Pd_2 \cdot 3(C_2H_3N)$
Formula Mass	394.78	381.75	1130.79
Crystal system	Monoclinic	Monoclinic	Triclinic
a/Å	8.9329(4)	10.5351(7)	11.1250(17)
b/Å	12.9165(6)	9.7782(6)	15.392(2)
c/Å	7.4073(4)	15.3104(10)	15.758(2)
α/°	90.00	90.00	74.695(3)
β/°	96.0390(10)	90.5550(10)	77.903(3)
γ/°	90.00	90.00	70.463(3)
Unit cell volume/Å^3	849.92(7)	1577.12(18)	2430.9(6)
Temperature/K	110(2)	110(2)	110(2)
Space group	*P2(1)/c*	*P2(1)/n*	$P\bar{1}$
No. of formula units per unit cell, *Z*	2	4	2
No. of reflections measured	9460	17456	24776
No. of independent reflections	2456	4560	11912
R_{int}	0.0177	0.0311	0.0307
Final R_1 values ($I > 2\sigma(I)$)	0.0207	0.0280	0.0387
Final $wR(F^2)$ values ($I > 2\sigma(I)$)	0.0520	0.0595	0.0932
Final R_1 values (all data)	0.0254	0.0371	0.0507
Final $wR(F^2)$ values (all data)	0.0544	0.0626	0.0993

Table 3. X-data for complexes: [Pd(OAc)(C^N)PPh_3] (**7**) and [Pd(*N*-Hpap)$_2$(NO_2)$_2$] (see also section 6.1.3.).

Compound reference	ijf1042 (**7**)	ijsf1110 [Pd(*N*-Hpap)$_2$(NO_2)$_2$]
Chemical formula	$C_{40}H_{38}NO_6PPd \cdot CH_2Cl_2$	$C_{38}H_{42}N_6O_{12}Pd \cdot 2(C_2H_3N)$
Formula Mass	851.01	963.28
Crystal system		
a/Å	47.4181(14)	8.4350(6)
b/Å	11.0136(3)	10.2678(5)
c/Å	17.7382(6)	13.5105(7)
α/°	90.00	77.953(4)
β/°	107.608(3)	76.502(5)
γ/°	90.00	72.666(5)
Unit cell volume/Å^3	8829.7(5)	1073.86(11)
Temperature/K	110.15	109.9
Space group	*C*12/*c*1	$P\bar{1}$
No. of formula units per unit cell, *Z*	8	1
No. of reflections measured	42881	16540
No. of independent reflections	7832	6809
R_{int}	0.0332	0.0315
Final R_1 values ($I > 2\sigma(I)$)	0.0373	0.0367
Final $wR(F^2)$ values ($I > 2\sigma(I)$)	0.1018	0.0919
Final R_1 values (all data)	0.0407	0.0399
Final $wR(F^2)$ values (all data)	0.1038	0.0942

6.1.3 X-ray structure of [Pd(*N*-Hpap)$_2$(NO_2)$_2$]

The complex, Pd(*N*-Hpap)$_2$(NO_2)$_2$], was isolated from a reaction of complex **6** with $NaNO_2$ in refluxing CH_3CN (a single crystal was picked from the bulk material).

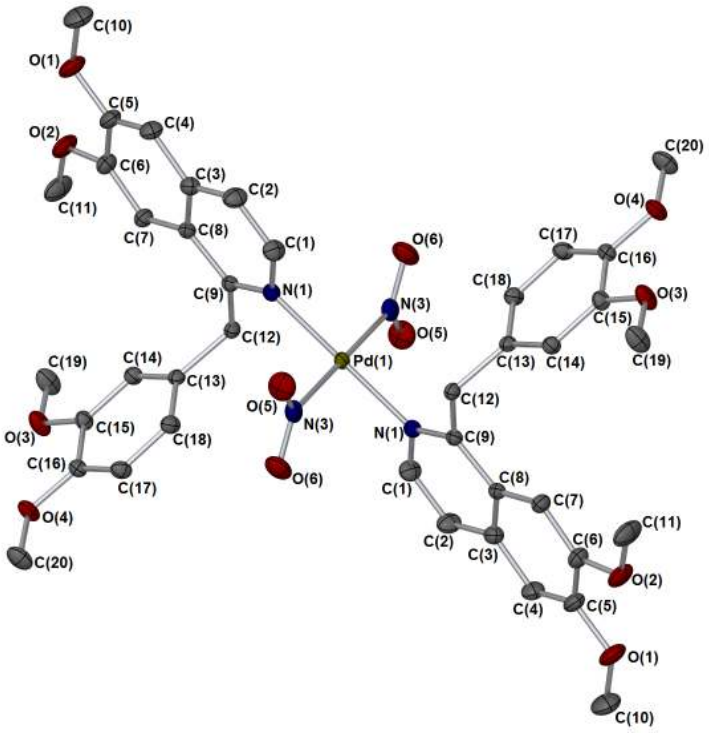

Figure 21. X-ray structure of Pd(*N*-Hpap)$_2$(NO_2)$_2$. 2 Molecules of CH_3CN removed for clarity. Thermal ellipsoids are set at 50%.

6.1.3.1 Proposed (tentative) mechanism to account for formation of Pd(*N*-Hpap)$_2$(NO$_2$)$_2$

The formation of Pd(*N*-Hpap)$_2$(NO$_2$)$_2$ from complex **6** requires some explanation. We did speculate that **6** may not have formed fully, leaving Pd(*N*-Hpap)$_2$(OAc)$_2$ as an initially formed complex prior to palladacycle formation. However, we have so far been unable to independently prepare Pd(*N*-Hpap)$_2$(OAc)$_2$ (an obvious precursor to Pd(*N*-Hpap)$_2$(NO$_2$)$_2$ by reaction of Hpap with Pd(OAc)$_2$). On this basis a tentative mechanism which may explain the formation of Pd(*N*-Hpap)$_2$(NO$_2$)$_2$ is given in the Scheme below. Further studies are underway to independently prepare this complex, allowing its full characterisation to be accomplished and chemical reactivity to be assessed.

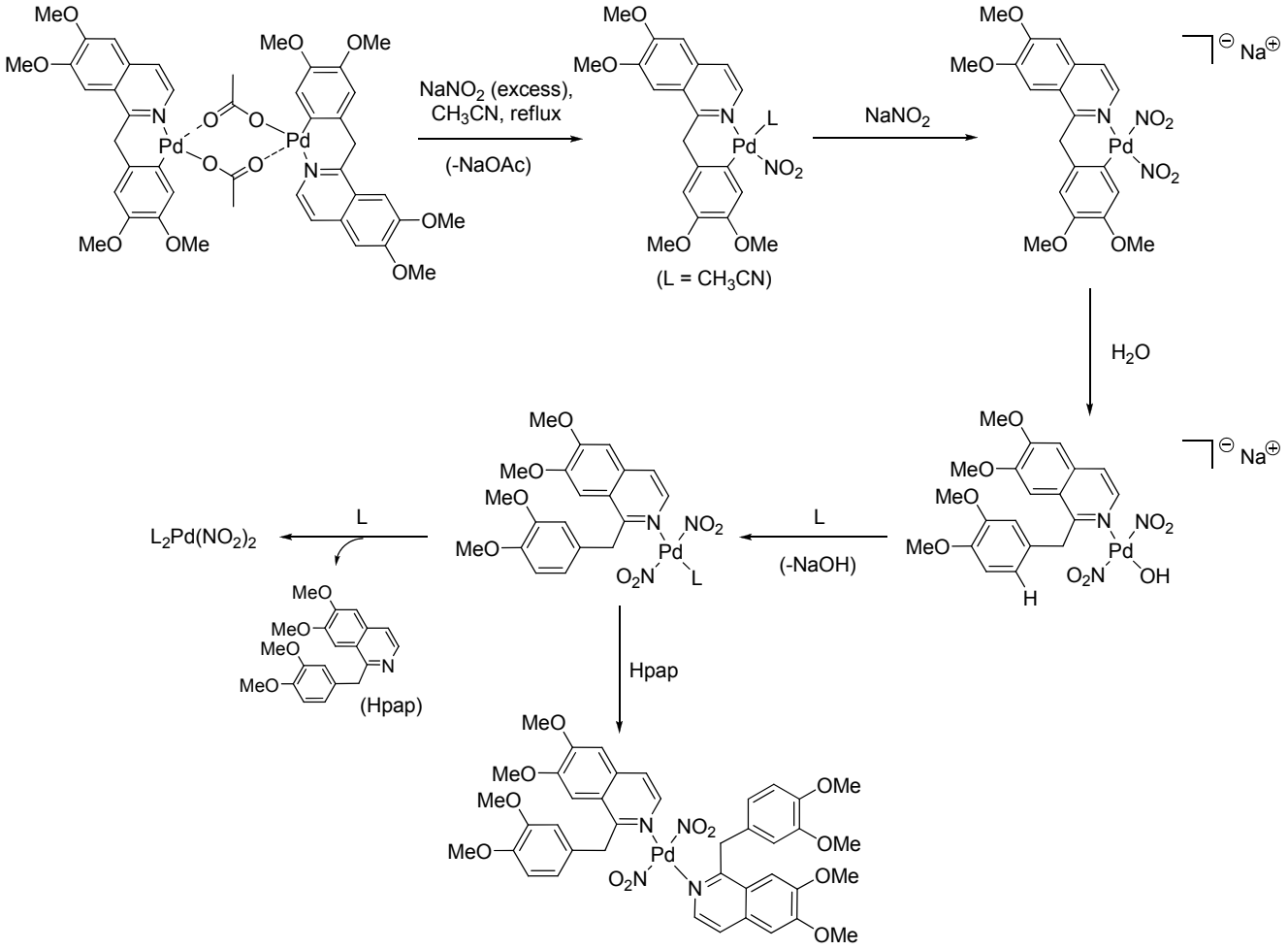

Scheme 1. Proposed mechanism explaining the formation of Pd(*N*-Hpap)$_2$(NO$_2$)$_2$.

6.2. Crystallographic data for compound 8 (crystallographic experiments conducted by Bath investigators)

X-ray diffraction studies on complex **8** were conducted on beamline I19 at the Diamond Light Source, Rutherford Appleton Laboratory, UK and on Station 11.3.1 of the Advanced Light Source, Lawrence Berkeley National Laboratory, California, USA. Single crystal data collections at

Diamond were carried out on a Rigaku Saturn CCD diffractometer equipped with an Oxford Cryosystems Cobra cryostream, while at the ALS data were collected using a Bruker APEXII CCD diffractometer equipped with a Oxford Cryosystems Cryostream Plus.

In photocrystallographic experiments a suitable single crystal was mounted on the diffractometer and flash cooled to 150 K. A ground state structure (GS) was first collected in the absence of any external light. The crystal was then irradiated *in-situ* at 150 K using a specifically designed LED ring, positioning six 400 nm LEDs (350 mcd, 3.7 V, 20 mA) 1 cm from the crystal in a uniform circle. In addition, the crystal was continuously rotated during this exposure to ensure maximum uniformity of irradiation. After 1 h irradiation the LED ring was removed and a second identical data collection conducted in the absence of light, from which the photoexcited structure was determined. The level of photoexcitation in the system was assessed through structure solution, with the conversion level for the isomers **8a** and **8b** refined using a disorder model in which the total occupancy of each atom was summed to unity. The process of irradiation, data collection, structure solution and refinement was then repeated to confirm that maximum conversion to **8b** had been achieved. The crystal was then held at 150 K in the dark for 1 h and a subsequent data collection confirmed that the level of photo-conversion remained unchanged, proving the excited state to be metastable at this temperature. Variable temperature parametic studies were then conducted in which the temperature was increased and identical datasets collected at intervals to determine the temperature range over which the metastable state was present.

In thermal crystallographic experiments a suitable single crystal was first mounted at room temperature on the diffractometer and a dataset collected in the absence of any light. The structure was solved and refined to determine the ratio of **8a** and **8b** isomers in the crystal, before the temperature was decreased at a rate of 120 K / h to slowly cool the crystal *in-situ*. Cooling was paused and identical datasets collected at regular intervals of *c.a.* 50 K and the structures were solved and refined in order to monitor any difference in the **8a**:**8b** ratio as a result of the temperature change.

The programs CrystalClear and APEXII were used for collecting frames, indexing reflections and determination of lattice parameters at Diamond and the ALS respectively, and the program SADABS was used for absorption correction at the ALS while CrystalClear was used to apply absorption corrections for the Diamond synchrotron data. The structures were solved by direct methods using SHELXS-86[12] and refined by full-matrix least-squares on F^2 using SHELXL-97.[13] In all the structures the ordered non-hydrogen atoms were refined with anisotropic displacement parameters, while disordered atoms were refined with occupancies summed to unity. Hydrogen atoms were placed in idealised positions and allowed to ride on the relevant carbon atoms. Refinements continued until convergence was reached.

Table 4. Details of the photoexcitation experiments with compound **8**.

Compound reference	8_GS150K	8_UV150K	8_VT200K
Chemical formula	$C_{39}H_{37}Cl_2N_2O_6PPd$	$C_{39}H_{37}Cl_2N_2O_6PPd$	$C_{39}H_{37}Cl_2N_2O_6PPd$
Formula Mass	837.98	837.98	837.98
Crystal system	Monoclinic	Monoclinic	Monoclinic
a/Å	10.7223(5)	10.7119(4)	10.7245(5)
b/Å	21.7779(13)	21.7420(12)	21.8948(15)
c/Å	16.3387(7)	16.4105(6)	16.3488(8)
α/°	90.00	90.00	90.00
β/°	105.321(4)	105.404(4)	105.251(5)
γ/°	90.00	90.00	90.00
Unit cell volume/Å^3	3679.6(3)	3684.7(3)	3703.7(4)
Temperature/K	150(2)	150(2)	190(2)
Space group	*P2(1)/c*	*P2(1)/c*	*P2(1)/c*
No. of formula units per unit cell, *Z*	4	4	4
Absorption coefficient, *μ*/mm^{-1}	0.743	0.742	0.738
No. of reflections measured	41375	40979	41224
No. of independent reflections	11231	11231	11279
R_{int}	0.0398	0.0380	0.0526
Final R_1 values ($I > 2\sigma(I)$)	0.0340	0.0328	0.0417
Final $wR(F^2)$ values ($I > 2\sigma(I)$)	0.0789	0.0771	0.1001
Final R_1 values (all data)	0.0429	0.0407	0.0546
Final $wR(F^2)$ values (all data)	0.0836	0.0814	0.1092
Goodness of fit on F^2	1.044	1.046	0.949

Table 5. Details of the slow cool experiments with compound **8**.

Compound reference	298K	250K	200K	150K
Chemical formula	$C_{39}H_{37}Cl_2N_2O_6PPd$	$C_{39}H_{37}Cl_2N_2O_6PPd$	$C_{39}H_{37}Cl_2N_2O_6PPd$	$C_{39}H_{37}Cl_2N_2O_6PPd$
Formula Mass	837.98	837.98	837.98	837.98
Crystal system	Monoclinic	Monoclinic	Monoclinic	Monoclinic
a/Å	10.786(8)	10.7248(5)	10.7075(7)	10.6878(7)
b/Å	22.362(17)	22.0346(11)	21.8698(14)	21.7334(14)
c/Å	16.405(12)	16.3099(8)	16.3273(10)	16.3349(10)
α/°	90.00	90.00	90.00	90.00
β/°	104.945(9)	105.1660(10)	105.3090(10)	105.4190(10)
γ/°	90.00	90.00	90.00	90.00
Unit cell volume/Å^3	3823(5)	3720.1(3)	3687.7(4)	3657.7(4)
Temperature/K	298(2)	250(2)	200(2)	150(2)
Space group	*P2(1)/c*	*P2(1)/c*	*P2(1)/c*	*P2(1)/c*
No. of formula units per unit cell, *Z*	4	4	4	4
Absorption coefficient, *μ*/mm^{-1}	0.715	0.735	0.741	0.747
No. of reflections measured	38082	39374	38982	39140
No. of independent reflections	11705	11236	11142	11046
R_{int}	0.0518	0.0560	0.0576	0.0793
Final R_1 values ($I > 2\sigma(I)$)	0.0465	0.0454	0.0455	0.0472
Final $wR(F^2)$ values ($I > 2\sigma(I)$)	0.1399	0.1312	0.1341	0.1207
Final R_1 values (all data)	0.0618	0.0606	0.0572	0.0563
Final $wR(F^2)$ values (all data)	0.1521	0.1408	0.1422	0.1262
Goodness of fit on F^2	1.004	0.988	1.006	1.071

6.3. CCDC reference numbers

CCDC reference numbers 858649-858660.

6.4. UV-vis spectroscopic analysis of [Pd(NO$_2$)(C^N)PPh$_3$] (8)

6.4.1. In solution

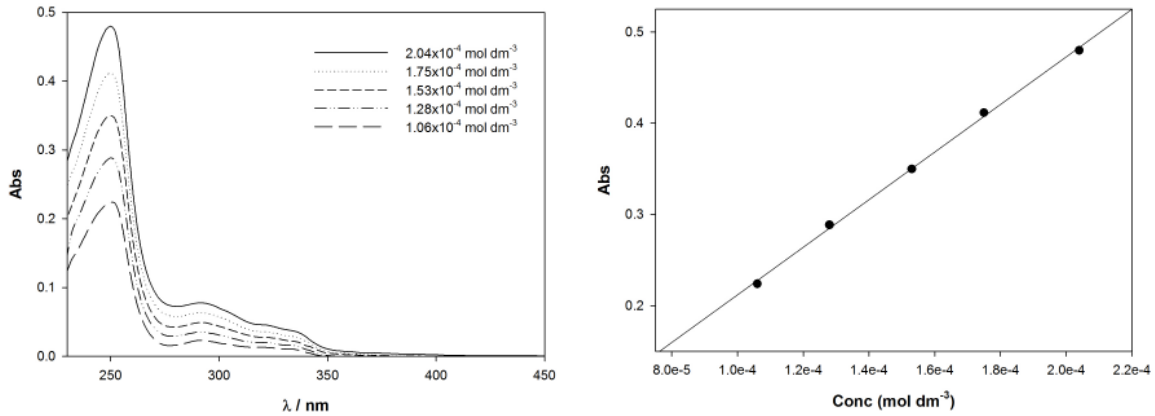

Figure 22: UV-vis spectroscopic data for [Pd(NO$_2$)(C^N)PPh$_3$] (**8**) in CH_2Cl_2 at 25 °C.

6.4.2. In the solid-state

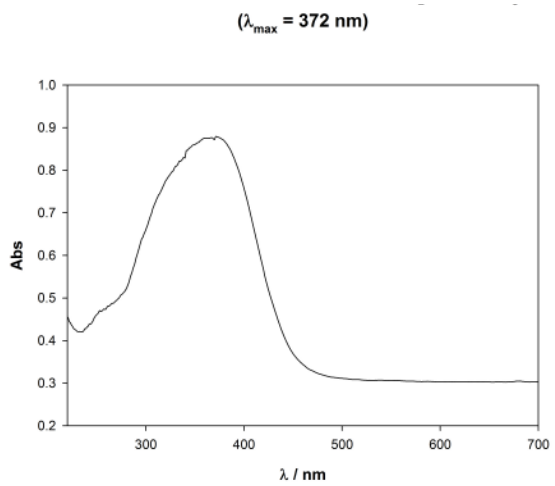

Figure 23: UV-vis spectroscopic data for [Pd(NO$_2$)(C^N)PPh$_3$] (**8**) (in the solid-state) at 25 °C. **Note:** the tail of absoption maxima extends into the visible region.

7.0. References

1. M. Walter, and L. Ramaley, *Anal. Chem.*, 1973, **45**, 165.
2. W. C. Still, M. Kahn, and A. Mitra, *J. Org. Chem.*, 1978, **43**, 2923.
3. T. E. Storr, C. G. Baumann, R. J. Thatcher, S. De Ornellas, A. C. Whitwood, and I. J. S. Fairlamb, *J. Org. Chem.*, 2009, **74**, 5810
4. N. R. Deprez, D. Kalyani, A. Krause, and M. S. Sanford, *J. Am. Chem. Soc.*, 2006, **128**, 4977.
5. J. Catalan, E. Mena, F. Fabero, and F. Amat-Guerri, *J. Chem. Phys*., 1991, **96**, 2005.
6. M. Nonoyama, *Synth. React. Inorg. Met. -Org. Chem.*, 1999, **29**, 119.
7. "SMART" - control software Bruker SMART Apex X-ray Diffractometer. v5.625, Bruker-AXS GMBH, Karlsruhe, Germany.
8. "SAINT+" - integration software for Bruker SMART detectors. v6.45, Bruker-AXS GMBH, Karlsruhe, Germany.
9. "SADABS" - program for absorption correction. v2.10. Sheldrick, G. M. Bruker AXS Inc., Madison, Wisconsin, USA, 2007.
10. "SHELXS-97" - program for structure solution. Sheldrick, G. M. University of Göttingen, Göttingen, Germany, 1997.
11. "SHELXL-97" - program for the Refinement of Crystal Structures. Sheldrick, G. M. University of Göttingen, Göttingen, Germany, 1997.
12. G. M. Sheldrick, *Acta Crystallogr., Sect. A,* 1990, **46**, 467.
13. G. M. Sheldrick, *Acta Crystallogr., Sect. A,* 2008, **64**, 112.